2020

PROTEOMIC ANALYSIS OF FETAL RAT NEURAL STEM CELLS AFTER TREATMENT WITH Hericium erinaceus

Bright Adam Test
University of the Pacific

PROTEOMIC ANALYSIS OF FETAL RAT NEURAL STEM CELLS AFTER TREATMENT WITH *Hericium erinaceus*

By

Bright A. Test

A Thesis Submitted to the

Graduate School

In Partial Fulfillment of the

Requirements for the Degree of

MASTER OF SCIENCE

College of the Pacific
Biological Sciences

University of the Pacific
Stockton, California

2020

PROTEOMIC ANALYSIS OF FETAL RAT NEURAL STEM CELLS AFTER TREATMENT WITH *Hericium erinaceus*

By

Bright A. Test

APPROVED BY:

Thesis Advisor: Craig Vierra, Ph.D.

Committee Member: Doug Weiser, Ph.D.

Committee Member: Lisa Wrischnik, Ph.D.

Department Chair: Eric Thomas, Ph.D.

PROTEOMIC ANALYSIS OF FETAL RAT NEURAL STEM CELLS AFTER TREATMENT WITH *Hericium erinaceus*

By

Bright A. Test

DEDICATION

This thesis is dedicated to my loving family. Thank you for your unconditional love and support. I will forever be especially grateful to you, mama and papa.

ACKNOWLEDGEMENTS

This thesis would not have been possible without the mentorship and support from the Vierra lab. Everyone contributed to a healthy and positive environment that allowed me to work at my best. Not a stale day went by as I chugged away to complete my thesis.

Most importantly, an infinite amount of thanks to Dr. Craig Vierra. Without his guidance and insight, I would not have been able to complete this project. I am forever grateful for his help and friendship.

PROTEOMIC ANALYSIS OF FETAL RAT NEURAL STEM CELLS AFTER TREATMENT WITH *Hericium erinaceus*

Abstract

By Bright A. Test

University of the Pacific
2020

The fungus, *Hericium erinaceus*, has outstanding chemical properties, displaying health benefits in digestive, hepatic, and nervous tissues. Its ease of accessibility and use makes it one of the most common substances used for treatment in Eastern medicine. More and more recent research is confirming the incredible health benefits of this fungus, especially the impact that is seen on nervous tissue growth and recovery post-treatment. Such neurite outgrowth and myelin sheath regeneration could illustrate the beginning of the cure to lifelong neurodegenerative diseases such as Multiple Sclerosis. In this first-of-its-kind study, we cultured and differentiated fetal rat neural stem cells while treating the samples with varying concentrations of aqueous extract of *Hericium erinaceus* mycelium. The cells were then harvested and lysed at various time points as the proteins were isolated and purified prior to analysis by LC-ESI mass spectrometry. A proteomic analysis was conducted where statistically significant changes in protein expression were observed between the control groups and the treated trials of both time points. While our initial targets of interest were not found, an up to 4-fold increase in protein expression was seen in a group of Histone H1 variants following treatment with *Hericium erinaceus*. These Histone H1 variants are known to be linker histones which interact with the core histone bead and play a role in chromatin remodeling. It is clear that *Hericium erinaceus*

plays a role in increasing the protein expression of Histone H1 variants which could lead to downstream effects yet to be revealed. This exploratory research should serve as a helpful launching point for those determined to understand the underlying mechanisms behind this phenomenon and the results it may have on the nervous system.

TABLE OF CONTENTS

LIST OF TABLES

Table

LIST OF FIGURES

Figure

LIST OF ABBREVIATIONS

cDNA	complementary DNA
CNS	Central Nervous System
DDT	dithiothreitol
DNA	deoxyribonucleic acid
IAA	indole-3-acetic acid
LC-ESI	liquid chromatography - electrospray ionization
µg	microgram
µL	microliter
MBP	myelin basic protein
mg	milligram
mL	milliliter
mm	millimeter
MS	Multiple Sclerosis
MS/MS	tandem mass spectrometry
ng	nanogram
NGF	nerve growth factor
NSC	neural stem cells
PNS	Peripheral Nervous System
RNA	ribonucleic acid
RT-qPCR	reverse transcription quantitative polymerase chain reaction

CHAPTER 1: INTRODUCTION

The nervous system is arguably the most complex biological system in our body. There are many different types of cells and molecules that play vital roles in maintaining the health and wellbeing of the system. In vertebrates, the nervous system is divided into two categories: the central nervous system (CNS) and peripheral nervous system (PNS). The CNS is composed of the brain and spinal cord, whereas the PNS consists of the peripheral nerves and ganglia that stem from the brain and spinal cord. There are two different cell categories in the nervous system, which include neurons and neuroglia (glia). Neurons are the nerve cells that send electrical signals, known as action potentials, throughout the human body which control muscle cell contraction and relaxation. Glial cells are supporting cells that play auxiliary roles and keep the overall environment healthy and proper for the neurons. Neurons can also be supported by neuropeptides known as neurotrophic factors. There are many neurotrophic factors that are involved in the regulation of growth, maintenance, proliferation, and survival of nerve cells, but the most common one that supports the growth of certain target neurons is known as nerve growth factor (NGF). NGF plays a crucial role in a lot of nervous tissue development and is a subject of interest in many studies. After many years of research, various protein markers have been visualized and have been used to determine the developmental state of nervous tissue. During development, all nervous tissue begins as neural stem cells which then differentiate into a variety of different neuronal cell types. Nestin is the most widely known of these protein markers and is mostly only found in undifferentiated neural stem cells. Other markers include neuron-specific enolase and fibrillary acidic protein, which is commonly observed inside glia. These markers are typically visualized during the quantitative analysis stages of research[19].

While there are multiple kinds of neurons and glial cells, oligodendrocytes are the largest glial cells and play an irreplaceable role. Oligodendrocytes are glial cells in the central nervous system that generate myelin, an important sheath that is responsible for enveloping neurons and ensuring proper action potential propagation. They are aligned in rows between the nerve fibers of white matter and are close to the somata of neurons in gray matter. The cytoplasmic processes of oligodendrocytes typically extend to multiple axons at once and wrap themselves around the length of the axon until multiple lamellas are formed. These cells and the myelin they generate are presumed to be majorly affected in patients suffering from Multiple Sclerosis (MS).

Overview of Multiple Sclerosis

There are many neurological diseases in today's world that are currently not curable, one of which is Multiple Sclerosis. MS is a demyelinating disorder in which the immune cells invade the CNS to remove myelin debris, but overdo it and cause neuron and oligodendrocyte death which leads to physical, mental, and psychiatric impairment problems[1]. White matter infiltration by our nervous system's immune cells is the focal point of the pathology of MS[17]. The immune cells most responsible for the inflammatory processes that occur during the onset and progression of MS are CD4-positive T lymphocytes; however, monocytes, macrophages, neutrophils, and B lymphocytes are also involved. While it was previously thought that the human brain does not change much after the first stages of development, it is now common to come across research showing the brain demonstrating structural and functional plasticity throughout the course of human life. This brain plasticity is affected when these infiltrating immune cells secrete various factors that control and regulate neuronal function and signal formation in neuronal synapses[18]. While Multiple Sclerosis is not an inherently deadly disease, patients suffering from MS typically have a reduced life expectancy. Initially, non-durable

remyelination occurs which typically leads to neurological function recovery in the short-term. As time progresses, however, the pathological changes become dominated by widespread microglial activation associated with extensive and chronic neurodegeneration, the clinical correlate being progressive accumulation of disability[15]. Paraclinical investigations show abnormalities that indicate the distribution of inflammatory lesions and axonal loss, interference of conduction in previously myelinated pathways, and intrathecal synthesis of oligoclonal antibody[15]. Cellular and secretory activity of infiltrating leukocytes contributes to the creation of these inflammatory demyelinated lesions in the white matter of the brain. The gray matter of patients with MS is also affected, leading to motor, sensory, visual, and cognitive impairment with the ability to memorize and learn being severely impacted[18]. MS is a chronic condition that cycles between relapses and remissions. The remission periods can last up to years, but symptoms flare up again eventually. Multiple Sclerosis is sometimes more specifically referred to as Relapsing-remitting MS because of this.

The current immunotherapies inhibit further demyelination, but do not act to enhance remyelination[1]. Licensed disease-modifying agents reduce the frequency of new episodes but do not reverse fixed deficits and have questionable effects on the long-term accumulation of disability and disease progression[15]. These treatments are also very expensive. The cost-effectiveness of a few disease-modifying drugs from a US societal perspective was analyzed and the results illustrated that dimethyl fumarate was the most preferred therapy to manage relapsing-remitting multiple sclerosis[3]. In 2014, the average annual medication cost of dimethyl fumarate was about $47,718[16]. Between 2011 and 2015, the annual disease-modifying therapy (DMT) cost per MS patient increased from $26,772 to $43,606, a 13.0% average annual growth rate[16]. When comparing DMT users to non-DMT users, the annual health care cost per DMT user was

74% higher in 2011 ($50,352 vs $28,881), increasing to more than double in 2015 ($70,683 vs $29,821)[16]. In the United States, the prevalence of MS has been presumed to be approximately 100/100,000 people[2]. Baldassari et al. describes in great length the therapeutic strategies being developed to promote myelin repair[22]. Almost all cells in the nervous system are potential targets as drug manufacturers try to modulate cellular activity and environment to promote myelination and to inhibit demyelination. There have been several laboratories that identified compounds which promote endogenous oligodendrocyte progenitor cell (OPC) function. Mesenchymal stem cell transplantation, high-dose biotin treatment, and protein pathway blocking are treatment methods that have been tested and are currently being explored some more due to the difficulty of successful implementation and monitoring *in vivo*. Other drugs such as dopamine antagonists, atypical antipsychotics, thyroid hormone inducers, and testosterone stimulators are also currently being investigated in clinical trials for remyelination potential in MS. Baldassari's group also describes multiple methods of screening and assessing myelin integrity: positron emission tomography, magnetization transfer imaging, myelin water imaging, and diffusion tensor imaging. There are also indirect ways of measuring myelin integrity: neurite orientation dispersion and density imaging, functional MRI, and magnetic resonance spectroscopy. These forms of measurement will become more accurate as the field focuses more on repairing myelin instead of simply trying to halt demyelination, but as of right now, the major difficulties involve lack of accurate biomarkers and lack of specificity when tracking affected myelin. It is important to fully understand the mechanism of action of remyelinating agents and their long-term safety and reliability before applying such advances to clinical care[22].

Chemical Properties and Effects of *Hericium erinaceus*

There may be a cheaper and more effective alternative on the horizon hiding inside a fungus. *Hericium erinaceus* (HE), also known as Lion's Mane, is a medicinal mushroom that contains neurotrophic and neuroprotective properties and has been widely consumed in Asian countries such as China and Japan[4]. The first account of this mushroom being consumed dates back to 264 A.D. on Taiwan Island where the natives ate *houtougeng* (translated to monkey head thick soup) and considered the soup to be beneficial in neutralizing the ill-effects of alcoholic beverages[5]. This mushroom is widely found in Asia, Europe, and northern temperate latitudes where beech and oak trees grow[6]. Even with modern technology and transportation methods, there is an unfortunate lack of *H. erinaceus* consumption and utilization in North America. The American species, *H. americanum* is also not commonly consumed.

As any fungus, HE is composed of mycelium and fruiting bodies. The powder of this crushed mushroom must be boiled in hot water to successfully extract the active compounds responsible for the health benefits experienced when consumed. These active compounds come in many forms including hericenones, erinacines, and polysaccharides, to name a few. Hericenones are a group of aromatic compounds that have previously been found in the fruiting bodies of HE. There were multiple aromatic compounds in this category that were isolated and purified by multiple researchers and the studies also revealed some anticancer properties tied to these compounds[21]. Hericinones, however, failed to stimulate NGF gene expression in primary cultured rat astroglial cells and 1231N1 human astrocytoma cells[23]. Li et al. describes erinacines as groups of cyathin diterpenoids that show biological activities as stimulators of NGF synthesis[24]. To date, 15 erinacines (erinacines A-K and P-S) have been identified and further investigations have demonstrated that eight of them have various neuroprotective properties,

such as enhancing NGF release (erinacines A-I), reducing amyloid-β deposition, increasing insulin-degrading enzyme (IDE) expression (erinacines A and S), or managing neuropathic pain (erinacine E), while others are either being currently discovered or have different pharmacological activities[24]. Li's group concludes by stating that erinacine A is effective in reducing neurodegenerative disease-induced cell death, but because there have been no studies illustrating erinacine A's crossing of the blood-brain barrier, it is hard to say how effective this compound will prove to be when consumed orally. Beneficial polysaccharides have also been discovered and analyzed. A polysaccharide EP-1 isolated from HE mycelia culture demonstrated antioxidant activity and prevented oxidative stress induced by H_2O_2 through mitochondrial dependent apoptotic pathways in gastric mucosa epithelial cells[20]. A heteropolysaccharide (HEP-S) was isolated from the fruiting bodies of *Hericium erinaceus* and was observed to function as an immunostimulator to stimulate both the innate and adaptive immune responses in mouse cells[25].

H. erinaceus has been reported to illustrate incredible health benefits for the body's digestive, immune, circulatory, and nervous systems. Helicobacter pylori is a bacteria found in the stomach and is the main pathogenic factor of chronic gastritis, peptic ulcers, and adenocarcinoma of the distal stomach[7], but its growth can be inhibited by using ethanol extracts and ethyl acetate fractions of HE[8]. The exopolymer produced in submerged mycelial culture of HE has been shown to significantly reduce the plasma triglyceride, total cholesterol, low-density lipoprotein cholesterol, phospholipid, and liver total cholesterol level in rats, implying that it has hypolipidemic effects[9,10]. There is a plethora of benefits to the nervous system such as, but not limited to, peroneal nerve recovery after crush injury[11], coordination of neuron functions associated with complex neurodegenerative diseases[6], and enhanced myelination in mature

myelinating fibers[12]. Another study has also found that HE can activate the synthesis of nerve growth factor (NGF)[13]. The stimulation of this neurotrophic factor can be beneficial in increasing the neurite outgrowth in a nervous system trying to combat a neurodegenerative disease. Most importantly and according to a study cited by many, aqueous extract of this mushroom has been shown to improve and expedite the process of myelination in nerve cells[14]. This commonly cited study by Kolotushkina et. al. examined the effects of applying *H. erinaceus* extract to cultures of newborn WISTAR rat cerebellums. When this group added the extract to their cells, they noticed no drastic changes in the development of nerve and glial cells, but the number of lamellae in the myelin sheaths did increase at a faster rate during development than untreated groups[14]. This activity, in theory, can directly counter the demyelination of nerves as seen in patients with Multiple Sclerosis. There are not many studies that cover this subject which make it difficult to find other studies that concur with the findings of this one. To our knowledge, there were no studies completed beforehand analyzing the proteomic contents of nerve cells in vitro being treated with *Hericium erinaceus*. Proteome analysis of the mushroom itself was conducted recently where mass spectrometry was used to identify a total of 2543 unique proteins in the *H. erinaceus* genome[26]. We can use the information from this study to help in our proteomic analysis, but the change in protein levels of rat fetal neural cells after treatment of *H. erinaceus* remains to be analyzed for the first time. Therefore, analyzing the proteomic contents of these neural cells treated with this mushroom can lead to uncovering more details about the proteins involved in the aforementioned myelinating process.

Proteomics

Proteomics is the large-scale study of proteins and requires the use of a variety of techniques stemming from fields such as molecular biology, biochemistry, and genetics. One vital technique, known as mass spectrometry, is utilized when analyzing a large amount of proteins at once. After isolating, purifying, and breaking down the proteins of interest into smaller peptides, the sample is fed into a mass spectrometer where the now-accessible peptides are charged and turned into precursor ions through techniques like Electrospray ionization (ESI). Mass spectrometry is used to measure the mass-to-charge ratio of these ions that are pulled through the mass spectrometer machine by an oppositely charged current. These are measured by a mass analyzer to generate what is known as a MS1 spectrum. As the ions are analyzed, certain ones are pulled through the machine where they collide with inert gas and fragment into charged amino acids through a process called Higher-energy Collisional Dissociation (HCD). These fragments are analyzed a second time by either a different mass analyzer or the same one from before, generating a MS2 spectrum which we can further investigate using specific computer software. This information allows investigators to see exactly what peptides were recognized by the mass spectrometry, making it possible to match discovered peptides to large databases in an effort to map back to proteins of interest. The parameters for which precursor ions are sent to further dissociate are set on the machine's software before the run begins. The machine we used for our studies is known as the Thermo Scientific™ Orbitrap Fusion™ Tribrid™ mass spectrometer. This machine's mode of function and interior is further explained in a thorough paper published by Hebert and colleagues[27].

Purpose and Goal

This study aimed to analyze the proteome of neural stem cells after *H. erinaceus* extract treatment. The primary objective was to explore whether treatment of neuronal stem cells with *H. erinaceus* extract resulted in changes in gene expression profiles for proteins involved in the myelination synthesis pathway. In our studies, we demonstrated that treatment of rat neuronal stem cells with *H. erinaceus* extract did not upregulate the expression of myelin basic protein or myelin expression factor 2, two known markers associated with myelin biosynthesis. However, they did reveal increased expression of histone 1 variants, suggesting treatment of neuronal stem cells with *H. erinaceus* extract leads to alteration in chromatin remodeling and gene silencing, which may suggest associations with controlling the neuronal differentiation program.

CHAPTER 2: MATERIALS AND METHODS

Neural Stem Cell Differentiation and Sample Preparation

Rat Fetal Neural Stem Cells (Invitrogen™ N744-100) were expanded using T75 flasks. The T75 flasks were coated with a matrix consisting of CELLStart™ (Gibco™ A10142001) diluted 1:100 in D-PBS with calcium and magnesium. 560 mL of this matrix was made in total. 14 mL of this matrix was used to coat each flask which were then incubated at 37°C in a humidified atmosphere of 5% CO_2 in air for 1 hour before being stored until use. Two different solutions were made: one for expanding the cells and one for differentiating the cells. Cells were passaged using StemPro® NSC SFM complete medium consisted of KnockOut™ D-MEM/F-12 with StemPro® NSC SFM Supplement, EGF, bFGF, and GlutaMAX™-I (all from Gibco™ and ThermoFisher). A mixture of penicillin and streptomycin was added to prevent bacterial and fungal contamination. See Table 1 for the breakdown of concentrations. The same medium lacking EGF and bFGF was used to differentiate the cells at P2. The volume remained unchanged after removing these small amounts of growth factor. To begin with, 4 of the previously matrix-primed T75 flasks were coated with cells and 20 mL of complete medium in each. Each flask contained about 5×10^5 cells at this point. After letting the cells grow for 24 hours, the complete media was siphoned and replaced with fresh complete media to minimize the accumulation of cellular debris. The cells expanded for a total of 3 days in Passage 0. Photos were taken every day for three days using light microscopy (Leica DMI3000 B). After three days, two of the four T75 flasks were further expanded while the other two flasks were frozen and stored in liquid nitrogen. Cells were passaged according to the manufacturer's instructions, except for the centrifugation step where 400 × g was used instead of 300 × g (MAN0001642).

The cells were then distributed evenly and plated into 8 T75 flasks to begin P1. The same procedure was followed and progress was recorded every day by light microscopy. The P1 cells were allowed to approach confluency (2 days of growth) and these cells were split (P2). P2 cells were split into smaller 100mm × 20mm plates and these cells were used as separate trials during the analysis. 6 mL of complete medium was used per plate which contained about 0.8 mL of cells. Cells were expanded for 3 days while progress was recorded. Three plates were harvested prior to the addition of the differentiation media. These cells belonged to an undifferentiated neural stem cell group of trials. The rest of the plates underwent an exchange of media where the complete medium was exchanged for one lacking EGF and bFGF (other concentrations remained the same as these small amounts did not affect volume significantly). Different versions of the incomplete medium were made containing different concentrations of dissolved *H. erinaceus* mycelia (supplied by Real Mushrooms) to be used for the cultivation of the trials. The mushroom powder was weighed out and dissolved in the media lacking the growth factors. The amounts used and concentrations generated are listed in Table 2. All proportions remained the same. Every remaining plate was coated with 10 mL of the differentiation medium. The remaining plates were grouped into different trials with different timepoints. Three replicates of the negative control, low concentration, medium concentration, and high concentration groups were harvested after 3 days of differentiation. At this time, the media was exchanged for media containing the mushroom extract. 5 mL was siphoned off to prevent the cells from being exposed to air and 10 mL of fresh differentiation media was added. The remaining three replicates of each group were harvested after 7 days of differentiation. Light microscopy was used to record the progress of cell differentiation. All cells were harvested and washed using the same procedure per plate. 7 mL of media was transferred to a conical tube using a sterile pipette

and cells were washed with 5 mL of D-PBS lacking Ca^{2+} and Mg^{2+}. The D-PBS was aspirated off and 1 mL of accutase was added to each plate. Cells were rinsed with 4 mL of matching media which was then transferred to the same conical tube. Cells were centrifuged at 400 × g for 4 minutes and the supernatant was discarded. The pellet was resuspended with 1 mL of cold D-PBS and spun again. This step was repeated once more and the resulting supernatant was removed. The cell pellet was frozen at -80°C. All cell subculturing protocols were carried out aseptically under a Laminar flow hood.

Table 1
Component Distribution for 100 mL StemPro® NSC SFM Complete Medium

Component	Concentration	Amount
KnockOut™ D-MEM/F-12	1X	97 mL
GlutaMAX™-I Supplement	2 mM	1 mL
bFGF	20 ng/mL	2 µg
EGF	20 ng/mL	2 µg
StemPro® NSC SFM Supplement	2%	2 mL
Penicillin + Streptomycin	0.5%	0.5 mL

Note. Table adapted from Invitrogen™ manual MAN0001642.

Table 2
Concentrations of H. erinaceus in 125 mL StemPro® NSC SFM Incomplete Medium

H. erinaceus Trial Name	**Concentration**	**Amount**
Low	0.1 mg/mL	12.5 mg
Medium	0.25 mg/mL	31.25 mg
High	0.5 mg/mL	62.5 mg

Peptide Purification

In-solution tryptic digestion was performed to prepare samples for mass spectrometer analysis. A total of 200 µL of 6 M urea/100 mM Tris buffer (pH 7.8) was used to lyse the cells. Sonication was also conducted as an additional measure to ensure complete cell lysis. To help denature proteins, 5 µL of reducing reagent, 200 mM DTT, was added and the sample was mixed by gentle vortex. After letting sit for 10 minutes in room temperature, 20 µL of alkylating reagent, 200 mM IAA, was mixed into the tube and vortexed. After another 10 minutes, 20 µL of 200 mM DTT was mixed in and allowed to sit for 10 minutes at room temperature. 775 µL of sterile MilliQ water was added to each sample to dilute the urea concentration and create an environment where trypsin can retain its activity. Initially, 3 µL of Trypsin Gold Solution (0.5 mg/mL) was added and the digestion was carried out overnight at 37°C. The next day, another 1.5 µL of Trypsin was added and allowed to digest for another 2 hours. The reaction was then stopped by adding 5.125 µL of 10% TFA.

Pierce™ C18 Spin Columns (Thermo Scientific™ No. 89873) were used to purify the samples. The columns were activated with 50% ACN, equilibrated with 5% ACN + 0.5% TFA solution, and used according to the manufacturer's instructions. About 1 mL of sample was bound, washed, and eluted. 20 µL of elution buffer was run through the columns twice to

guarantee a thorough product. This resulted in a 40 µL solution that would be stored and later used for analysis.

Colorimetric Peptide Assay and Normalization

Eighteen samples were analyzed by use of the Pierce Quantitative Colorimetric Peptide Assay (Thermo Scientific™ No. 23275). Prior to this analysis, these samples were lyophilized and then resuspended with 15 µL of 5% ACN + HPLC grade water + 0.1% Formic Acid solution. All reagents were made as per the manufacturer's instructions and the protocol was followed stringently. 2 µL of each sample was mixed with 18 µL of autoclaved water before being mixed with the 180 µL of working reagent. After running the software analysis, some discrepancies were visible between the biological replicates. In order to maximize the amount of peptide binding to the mass spectrometer analytical column, the biological replicates with the higher peptide concentration were selected. These samples were normalized with HPLC grade water + 0.1% Formic Acid to match the limiting concentration of one of the samples (the control for Day 3). The concentrations and samples selected are illustrated in Table 3. After randomizing the order in which they would be processed, the samples were inserted into the mass spectrometer to begin the proteomic analysis. Every sample was injected twice at a volume of 25 µL per injection, creating technical replicates. The second injections were treated as separate samples when it came to randomizing the order.

Table 3
Observed Initial Concentrations of Chosen Samples and Post-Normalization Values

Sample	Initial Concentration (µg/mL)	Concentration Needed (µg/mL)	Volume of Sample (µL)	Volume of Water Mixture (µL)
3C2	174.495	1.74495	10	40
7L1	200.901	1.74495	8.68	41.32
7H2	213.293	1.74495	8.18	41.82
3M2	236.433	1.74495	7.38	42.62
NSC2	250.005	1.74495	6.98	43.02
7M1	262.165	1.74495	6.65	43.35
3L2	324.988	1.74495	5.37	44.63
7C1	365.978	1.74495	4.77	45.23
3H1	438.012	1.74495	3.98	46.02
HeLa	155.022	-	20	80

Note. Samples are notated by the format of [Trial Day][Trial Group][Replicate Number]. For example, 3C2 is Day 3 Control no. 2. NSC2 refers to the undifferentiated Nerve Stem Cells sample used. HeLa cells were included to check for consistency during the Mass Spectrometry run every 24 hours. Water mixture consists of HPLC grade water + 0.1% Formic Acid. All samples except for the HeLa cells were injected twice (25 µL per injection). The HeLa cells were injected four times with the same amount of protein per injection.

Proteomic Analysis

Peptides were eluted from the C18 column and subject to electrospray ionization and the samples were analyzed using our Thermo Scientific™ Orbitrap Fusion™ Tribrid™ mass spectrometer. Individual samples were subject to approximately a 2 hr chromatographic run using a previously established X-calibur program. The entire running time on the mass spectrometer was about 72 hours. A sample of HeLa cells was injected every 24 hours to confirm spray stability of the needle during the run. The total volume of HeLa cells was divided into four injections for a total of 25 µL per injection. Once completed, chromatography graphs,

MS and MS/MS data were generated. Data were further analyzed through quantitative analytical software, such as Peaks Studio and Protein Scaffold 4.

RT-qPCR Analysis

In order to complete reverse transcription and quantitative polymerase chain reaction analysis (RT-qPCR), total RNA was isolated, washed, and solubilized. A standard Trizol RNA isolation procedure was done according to Invitrogen's manual (Pub.No. MAN0001271 B.0). All samples were lysed with Trizol containing 60 µL of 100% chloroform and centrifuged to generate separate phases within tubes. Each sample's aqueous phase was transferred to a new tube and precipitated using 150 µL of 100% isopropanol along with centrifugation at 4°C. The gel-like pellets that resulted were then washed three times 3 with 300 µL of 70% ethanol. After vacuum-drying the pellets for about 20 minutes, the pellets were resuspended in 20 µL of RNase-free water. The RNA yield for each sample was determined by use of the ThermoScientific™ NanoDrop 2000c Spectrophotometer and the appropriate absorbance values were recorded.

The purified RNA was then prepared for RT-qPCR analysis by mixing with the proper reagents from the PowerUp™ SYBR™ Green Master Mix (Applied Biosystems™). The RNA was first diluted to a concentration of 12.5 ng/µL. Then, the following mixture was produced: 4 µL of 12.5 ng/µL RNA; 10 µL of 2x SYBR green dye; 0.2 µL QN SYBR green Reverse Transcriptase mix; 1 µL of 20x primer mix; 4.8 µL RNase free water. Samples were analyzed for each of the five primers and technical duplicates were also generated. Forward and reverse primers were mixed (see Table 4) and checked for their ability to amplify their specific amplicon beforehand using 2% agarose gel electrophoresis. A 96-well plate was used to load 18 µL of each mixture and was then processed by the continuous fluorescence detector.

Table 4
Primer Sequences for Histone H1 Family

Histone Name	Forward 5’ to 3’	Reverse 5’ to 3’	Forward MT (°C)	Reverse MT (°C)
H1.1	gaagcctgcgaaagctgctgt	gaaactgcaggcttcttgggc	64	66
H1.2	gtcggaaactgctcctgctgc	ggcttggcctcgccagaagct	68	70
H1.3	ttgaaacatgtctgaaacagctcc	atgcggctgttgttcttctcc	68	64
H1.4	aagaagaaggcccgcaaggcc	ccgccttcttgttgagtttga	68	62
H1.5	aagaagaagacaaaaaaagctggc	cttagccttgggcttggcttc	66	68

Note. Melting Temperatures (MT) for both forward and reverse primers are shown. Primers are shown as 5’ to 3’.

CHAPTER 3: RESULTS

Neural Stem Cell Differentiation

Light microscopy was used to examine the process of growth and differentiation of the nerve stem cells. Photos were taken every day in greyscale and monitored for healthy progression. The Day 3 trial groups were compared to the Day 3 control and undifferentiated stem cells at Passage 2 (Figure 1). A visible difference between the morphology of the stem cells and the morphology of the differentiated cells was seen (Figure 1). The differentiated cells in both the control group and the trials seemed to successfully form neural connections typically seen in nervous tissue. The morphology of the cells from the trials did not seem to significantly deviate from the control group, illustrating that the addition of the *H. erinaceus* extract did not cause any significant changes to the physical appearance of the cells.

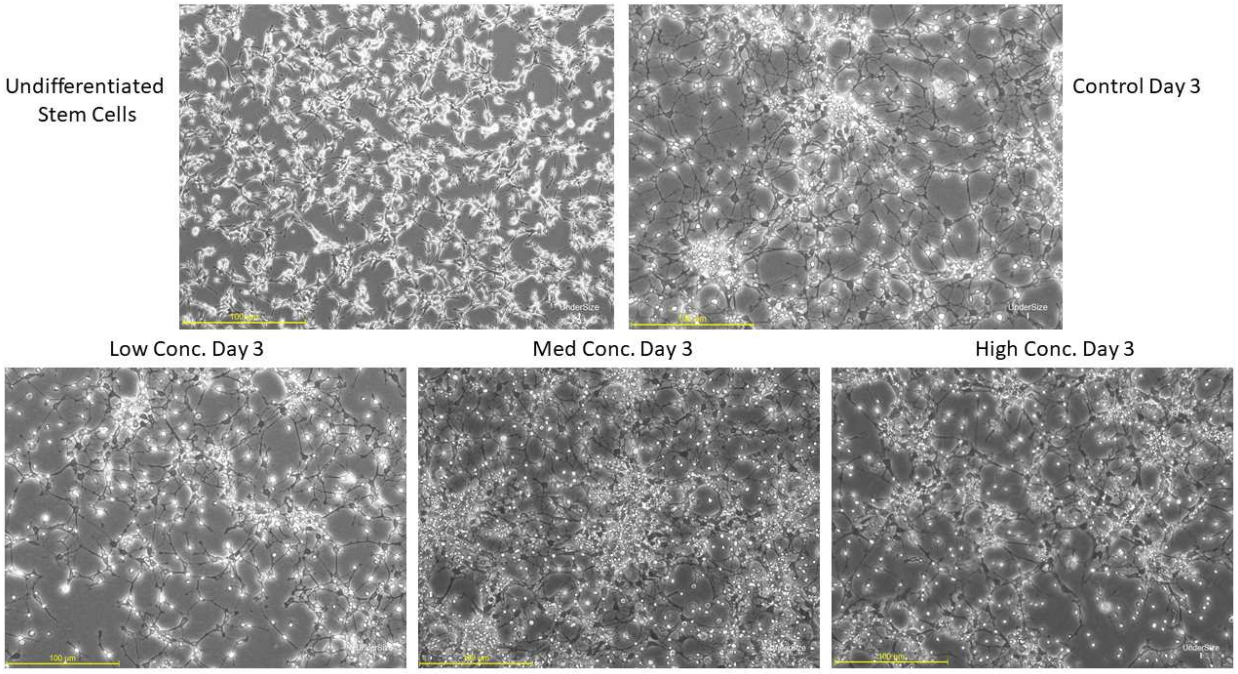

Figure 1. Comparison of morphology between undifferentiated stem cells and Day 3 Control and treatment groups using light microscopy. The yellow measurement bar is set to 100 µm for reference. The treated groups and undifferentiated stem cells are portrayed in 200x magnification while the Control group is portrayed in 100x magnification.

The same could not be said about the Day 7 group. In comparison to the Day 3 group, the Day 7 group illustrated more solid groupings of nerve cells and glia with more distinct crater-like low-density spaces in between the formations (Figure 2) illustrating a progression in maturation. A uniquely dense cluster of cells, similar to controls, was found when analyzing the Low Concentration trial for Day 7 as seen in Figure 2. When comparing the Day 7 trials, the ones that were treated with the medium and high concentrations of *H. erinaceus* exhibited what seemed to be less specific condensed grouping of cells which resulted in less crater-like low-density space compared to the low concentration and control trials, and which appeared to mimic the cells at Day 3 of treatment as opposed to untreated controls and low-dose treatments.

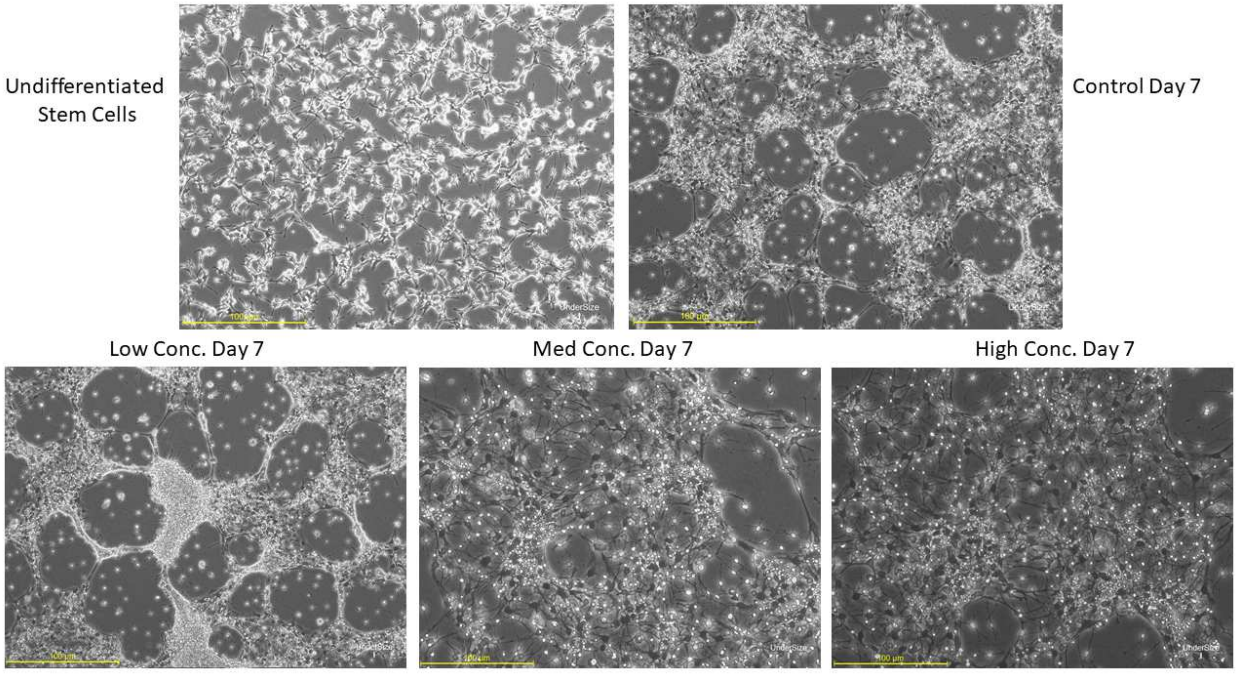

Figure 2. Comparison of morphology between undifferentiated stem cells and Day 7 control and treatment groups using light microscopy. The yellow measurement bar is set to 100 µm for reference. The treated groups and Control are portrayed in 100x magnification while the undifferentiated stem cells are portrayed in 200x magnification.

Proteomic Analysis and Mass Spectrometry

Prior to use for proteomic analysis, the grown cells from all samples were washed with D-PBS lacking Ca^{2+} and Mg^{2+} and detached at their respective time points with acutase, followed by cell lysis in urea. Following crude lysate collection and tryptic digestion, samples were purified using C18 spin columns and checked for peptide concentration using Colorimetric Peptide Assay. The initial concentrations were recorded (Table 3). After normalizing the concentrations to the baseline concentration of sample 3C2, samples were inserted into the mass spectrometer and analyzed over a 4 day period. Each individual sample was analyzed for about 2 hours. Chromatographic graphs were generated to illustrate the relative abundance of peptides eluting off of the column at every point in time. Similarities between retention time and relative abundance are best illustrated between the control and trial groups of the same day (Figure 3).

There are certain notable differences in the graphs, but for the most part, there is not much variation to be seen in the overall shape. This implies that the samples were handled and processed properly with little error. For the Day 3 group, there was a peak missing in 3C at roughly the 22.70 minute retention time that was visible in all the other trials in varying abundances (Figure 3). The Day 7 control group seemed to differ from the Day 7 treatment groups, most notably in the end of the chromatographic run around 91-94 minutes. There were a couple of peaks showing more abundance in the treated groups compared to the control, signifying that there may be proteins that are uniquely expressed and representative peptides are eluted off the column at that point that are not found in the control group. It may also be the case that those same peptides might have simply been eluted at a different point in a spread out way. This is unlikely, however, since by looking at the overall curve of the 7C graph, it is hard to spot where these peaks could have shifted to. Overall, these figures confirm our assertion that the samples analyzed display similar quantities of peptides, allowing us to carry on with further analysis using additional software.

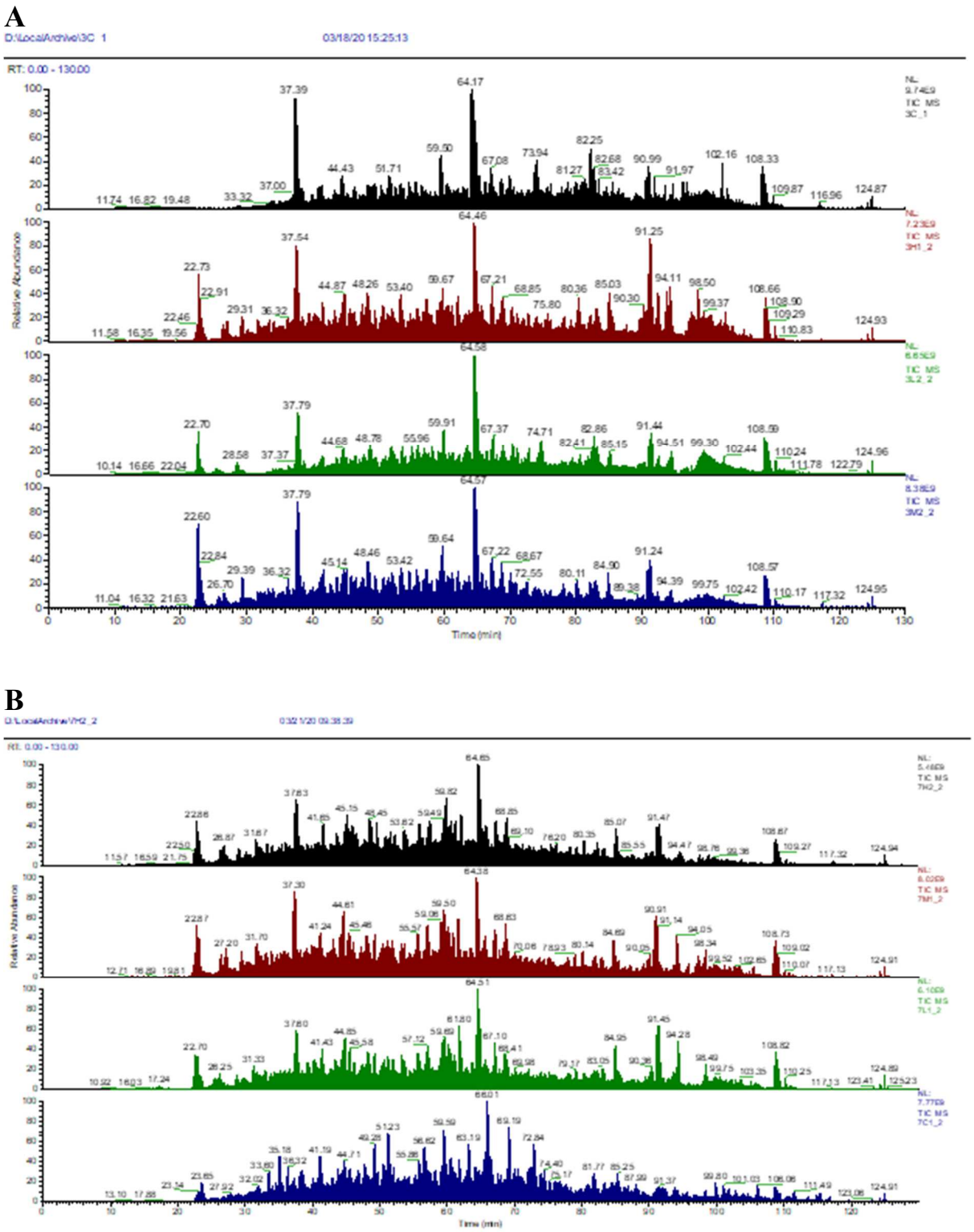

Figure 3. Raw chromatography files from the Thermo Scientific™ Orbitrap Fusion™ Tribrid™ mass spectrometer after completing the sample processing. These graphs compare the relative abundance of peptide (y-axis) to the retention time (x-axis). A: Day 3 Group color-coded and labeled. B: Day 7 Group color-coded and labeled. Note the difference in order from top to bottom between A and B.

Quantitative Proteomic Analysis

Mass spectrometry data were analyzed using Protein Scaffold (Proteome Software, Inc.™), a software algorithm designed for quantitative proteomics. Within this software algorithm, MS/MS spectra were tallied up and normalized in preparation for quantitative comparison and analysis. Protein sequences, statistical correlation, and probability percentages were illustrated among many other useful metrics. Prior to optimization, a total of 365,537 spectra were obtained from the combined 8 sets of data (Day 3 Control, Day 7 Control, Day 3 Low, Day 3 Medium, Day 3 High, Day 7 Low, Day 7 Medium, Day 7 High). The protein threshold value, minimum number of peptides value, and peptide threshold value were modified. As the software conducts the internal statistical analysis, it checks for the probability of a protein or peptide actually existing in the sample according to the registered and recognized spectra. The protein and peptide thresholds are in reference to these probabilities. For our analysis, protein and peptide thresholds were set to 95%, indicating that Scaffold would only display proteins and peptides that the algorithm calculated of having at least a 95% probability of being present in the samples. The minimum number of unique peptides used for protein identification was set to 2, which is commonly accepted by the proteomic community to confirm the presence of proteins. These parameters narrowed the results and allowed for a more stringent and accurate observation of proteins that were most likely to be "real". These parameters also minimized the false discovery rate and dramatically lowered the chances of encountering false positives in the data. After setting such parameters, there were a total of 648 unique proteins and 21,602 spectra found when comparing the Day 3 Control to the Day 3 Trial groups. A statistical two-tailed T-test was conducted and found that 61 of these proteins were statistically significant with a p-value of less than 0.05. Of these 61 proteins, 26 were expressed in higher quantities, up to a 4-fold difference,

in the Day 3 Control compared to the trials. The rest of the 35 proteins were expressed in lower quantities, up to a 4-fold difference, in the Day 3 Control compared to the trials (Appendix A). The same statistical analysis was conducted for the Day 7 groups where a total of 1042 unique proteins and 37,541 spectra were found following analysis using the same parameters. After finding 193 statistically significant proteins, 64 of them were expressed in higher amounts, up to a 4-fold difference, in the Day 7 Control compared to the trials. The other 129 proteins were expressed in lower quantities, up to a 4-fold difference, in the Day 7 Control compared to the trials (Appendix B). A final statistical analysis, ANOVA (p-value < 0.05), was conducted to illustrate significant variance between all three groups of trials (Controls vs Day 3 trials vs Day 7 trials). A total of 129 unique proteins across all samples were found to be statistically significant according to this analysis with respect to changes in protein expression (Appendix C). Of these proteins, 36 were unanimously expressed in higher amounts, up to a 4-fold difference, in the Day 3 and Day 7 trials when compared to the Control groups. On the other hand, 17 proteins were expressed in lower amounts, up to a 4-fold difference, in the Day 3 and Day 7 trials when compared to the Control groups. These proteins were researched one-by-one to find any correlation to previous studies about *H. erinaceus* or Multiple Sclerosis. While there were no statistically significant proteins found that have a direct role in either of these subjects, there was a profound change seen in the expression of certain histones between the control groups and the trial groups. There were multiple notable histones such as H2A, H1.1, H1.2, H1.3, H1.4, and H1.5. Most of these histones were variants of the H1 family. Differences in expression are visualized in Figure 4 where there was at least a 4-fold difference in normalized spectral counts between the control and trial groups. The largest differences are visualized in Figures 4B, 4C, and 4D. Simultaneously, the undifferentiated cells were compared to the controls to confirm that

differentiation was successful on a genotypic level. Nestin, a protein expressed at high levels in neural stem cells and a widely employed marker[28], was shown to be expressed less in the differentiated controls as illustrated in Figure 5.

A

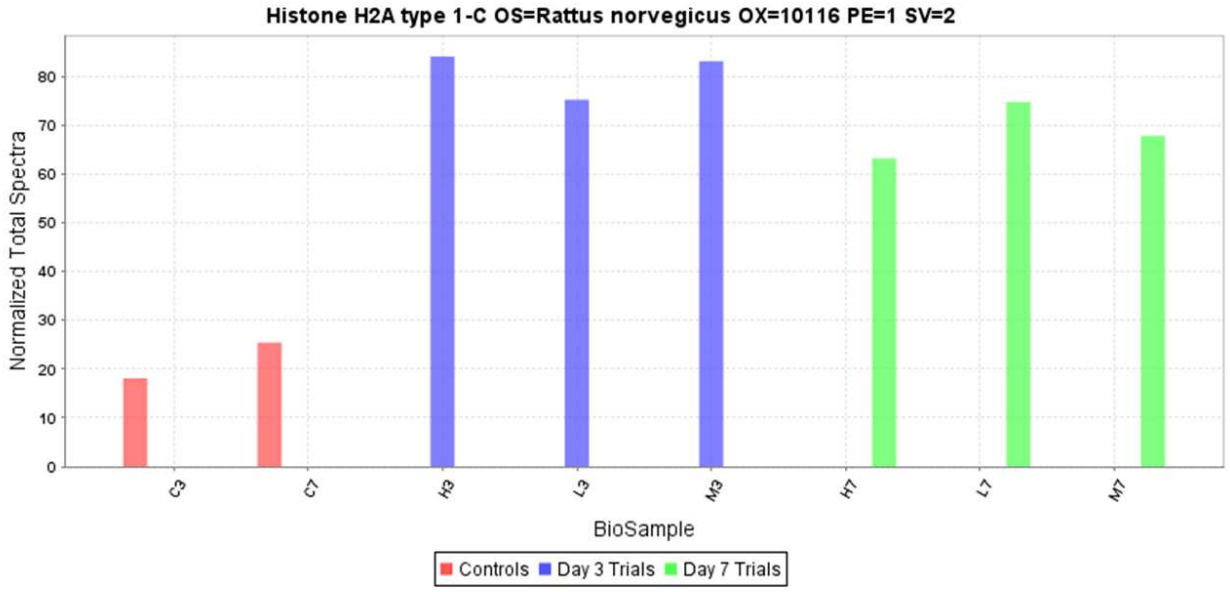
Histone H2A type 1-C OS=Rattus norvegicus OX=10116 PE=1 SV=2
Normalized Total Spectra
0
10
20
30
40
50
60
70
80
C3
C7
H3
L3
M3
H7
L7
M7
BioSample
Controls
Day 3 Trials
Day 7 Trials

B

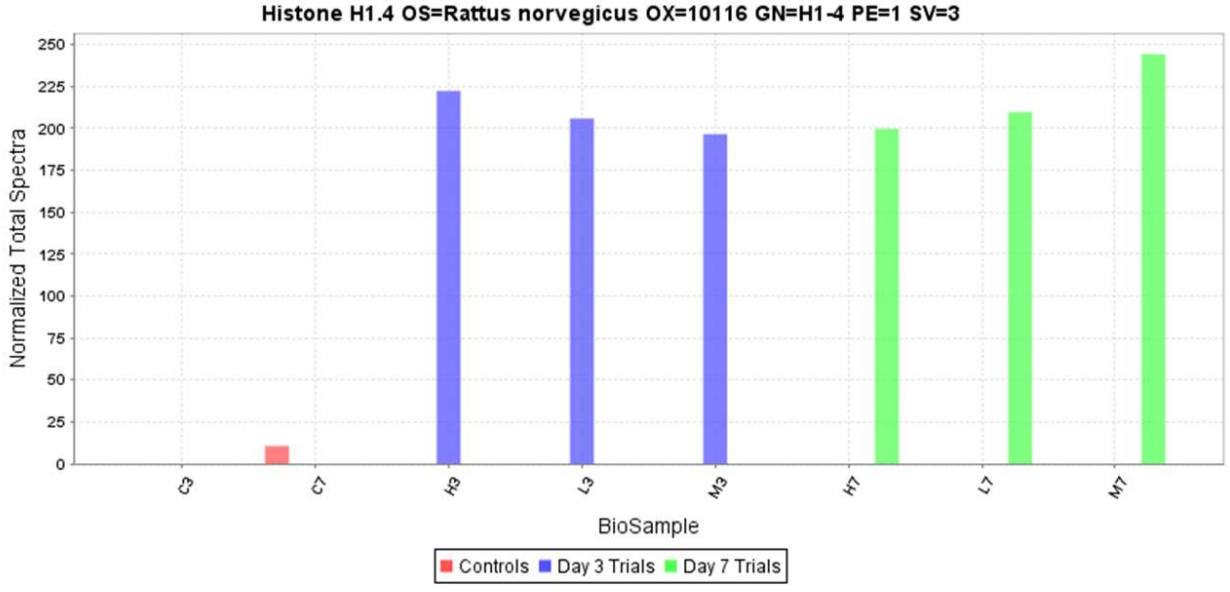
Histone H1.4 OS=Rattus norvegicus OX=10116 GN=H1-4 PE=1 SV=3
Normalized Total Spectra
0
25
50
75
100
125
150
175
200
225
250
C3
C7
H3
L3
M3
H7
L7
M7
BioSample
Controls
Day 3 Trials
Day 7 Trials

(Figure 4 Continued)

C

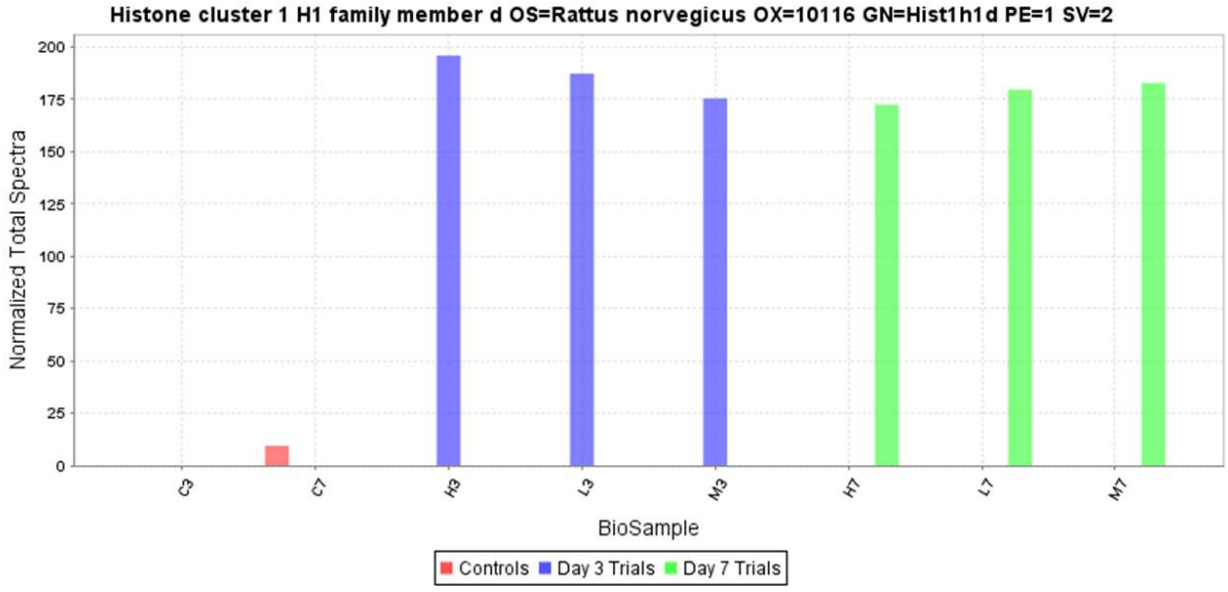

D

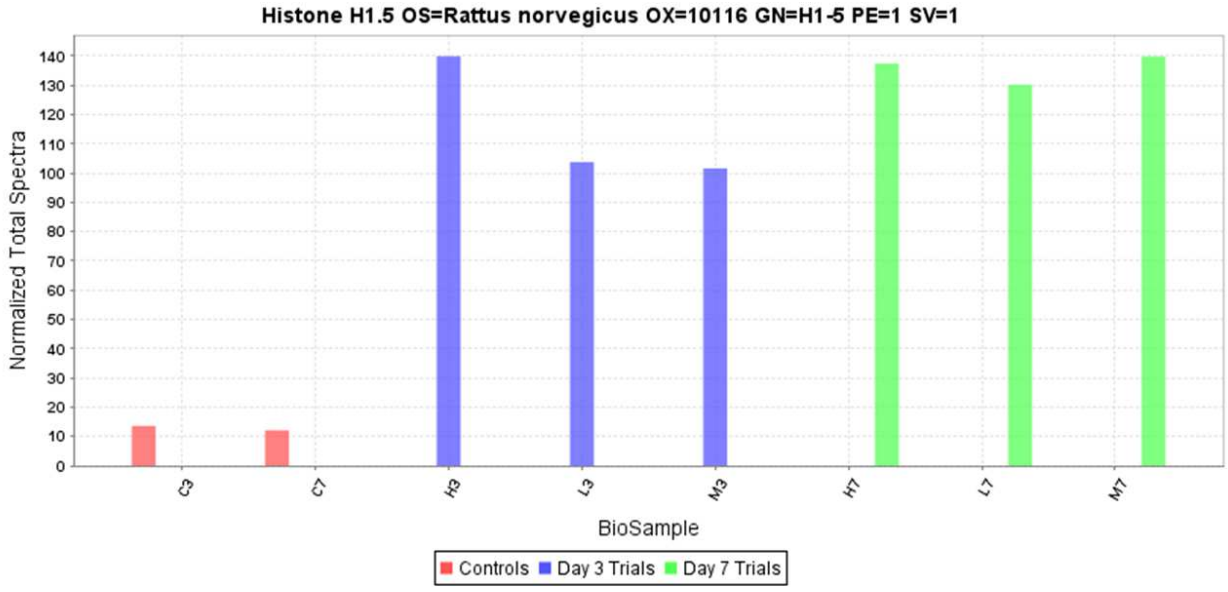

(Figure 4 Continued)

E

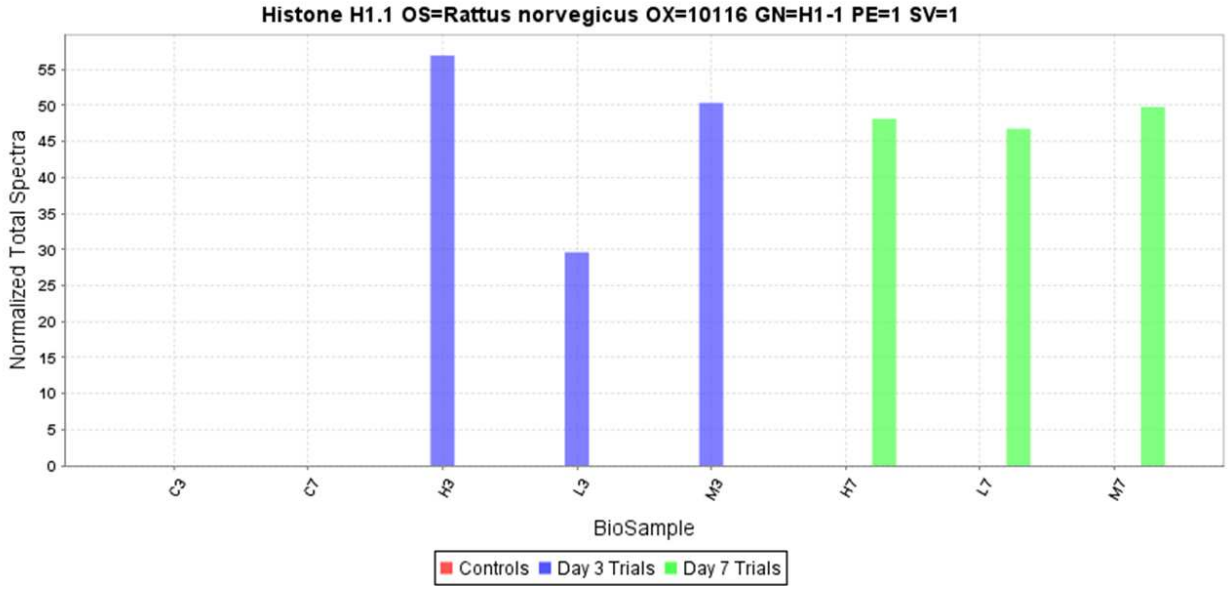

F

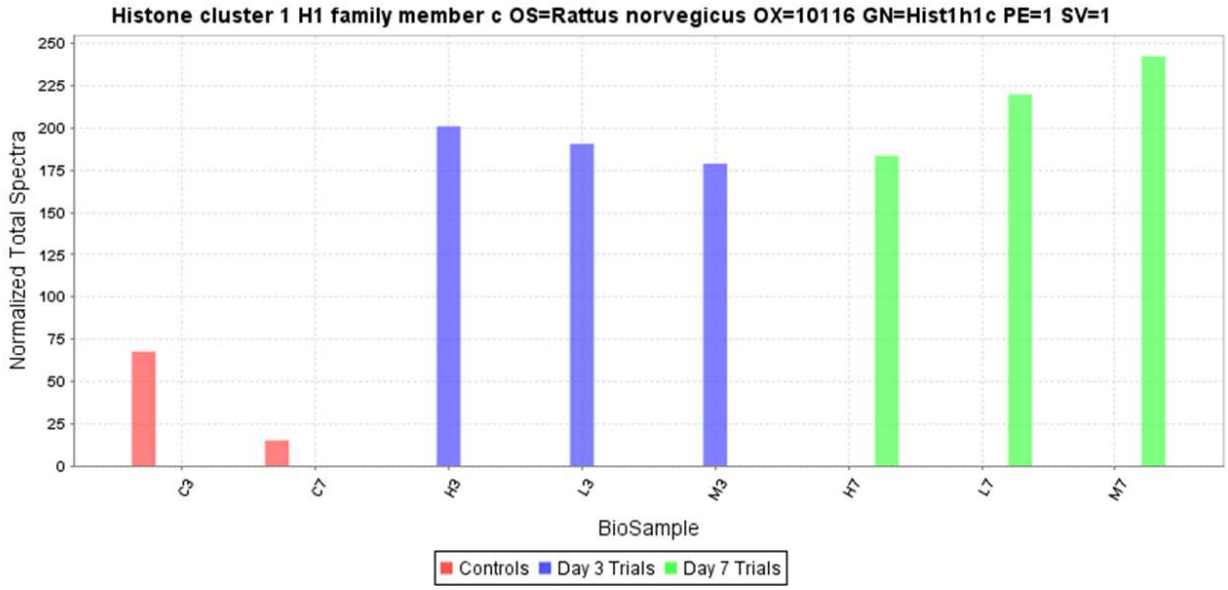

Figure 4. Normalized total spectra vs biosample. These graphs were exported as raw data from Protein Scaffold. The raw number of Total Spectra is not as important as the comparison in values and changes between the groups of samples. All histones significantly increased in expression when treated with *H. erinaceus*, regardless of elapsed days. A: histone H2A Type 1-C. B: histone H1.4. C: histone cluster 1 H1 family member d (histone H1.3). D: histone H1.5. E: histone H1.1. F: histone cluster 1 H1 family member c (histone H1.2).

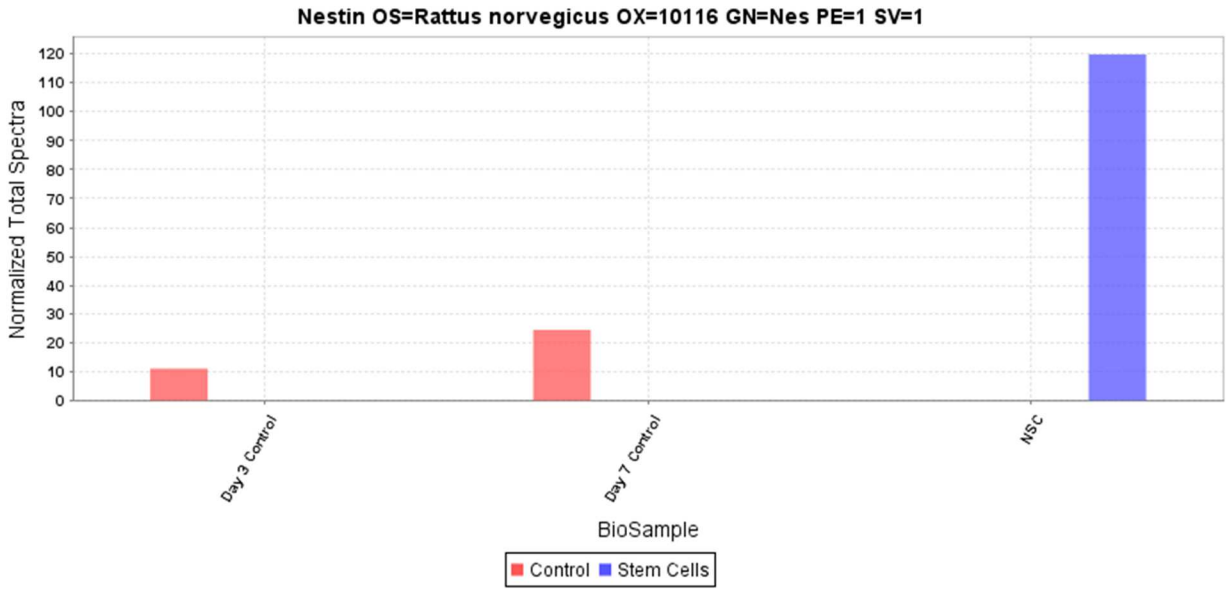

Figure 5. Normalized total spectra of nestin in controls vs nerve stem cells. The lower amount of spectral counts in the controls implies that less of the marker protein is expressed in these samples. Based on this evidence, differentiation did successfully occur.

The Protein Scaffold software also generated scatterplots after the ANOVA test was conducted (Figure 6). The control group (Day 3 Control and Day 7 Control) was compared to the Day 3 trials separately from the Day 7 trials. Both graphs illustrated a similar pattern when comparing averaged normalized total spectra. This demonstrated that there was little variation in the trials due to the different time points. As a result, however; there was a clear significant difference shown between the controls and the trials.

A

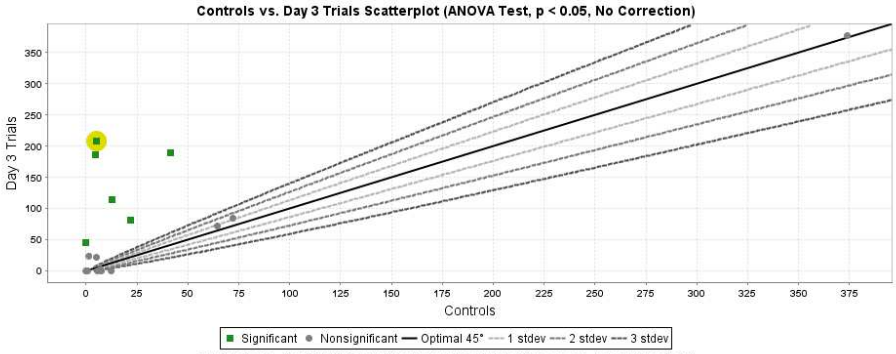

B

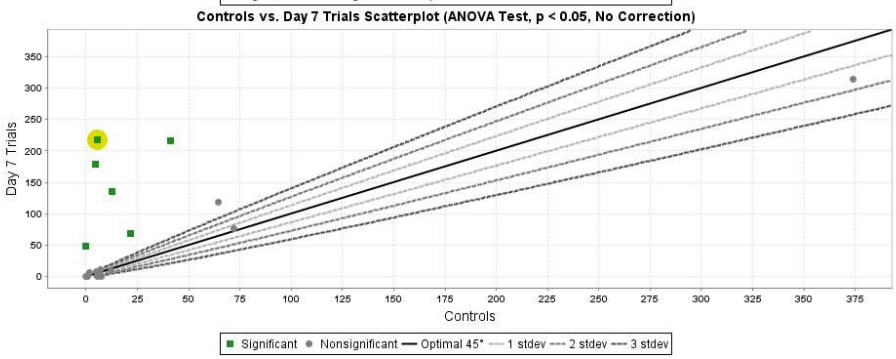

Figure 6. ANOVA test results of histones in controls vs trials. The highlighted green box in both A and B refer to histone H1.4 simply for reference. The numbers on both axes represent Total Normalized Spectra as an average in those groups. The green boxes represent a protein that significantly shows more normalized spectra in a trial group than a control group and vice-versa. In this case, the six green boxes refer to the histones in Figure 4.

The amino acid sequences of these proteins were also examined to see if there were any substantial differences in the order of amino acids that could further explain the specific function of these histone variants. As illustrated in Figure 7, all of the six examined histone variants were rich in both arginine and lysine with minor variation in overall charge. This was to be expected, as histones must use an overall positive charge to tightly bind to DNA when condensing it into chromatin.

Figure 7. Recognized peptide sequences matched with a proteome database and mapped back to the histones of interest. The amino acids highlighted in yellow are confirmed to match by available spectra data. All peptides from each protein were examined, but only the best-matched peptide from each protein was chosen to be compared.

Since we selected a neural cell line based on previous studies of myelin sheath regeneration being affected by *H. erinaceus*[14], it was useful to look for any proteins that could correlate our results to these previous studies. In our analysis, only one myelin related protein was found in every sample. This protein, known as Myelin expression factor 2, did not show any significant variation (ANOVA) in expression between the control group, the Day 3 trials, and the Day 7 trials (p-value = 0.34). The control for day 3 showed a drastically different result from the control for day 7 whereas the other groups did not show much variance within their respective groups. Based on this data, we cannot make any solid conclusions, but it was interesting to see the decrease in normalized total spectra when going from the Day 3 group to the Day 7 group. If it were true that Myelin expression factor 2 was being expressed less as time went on, then expression levels of myelin basic protein (MBP) would increase. This is because Myelin

expression factor 2 is a transcriptional repressor for MBP. MBP is one of the main components of myelin sheath so seeing an increase in expression of this protein would illustrate an increase in total myelination occurring. The normalized total spectra data is illustrated in Figure 8.

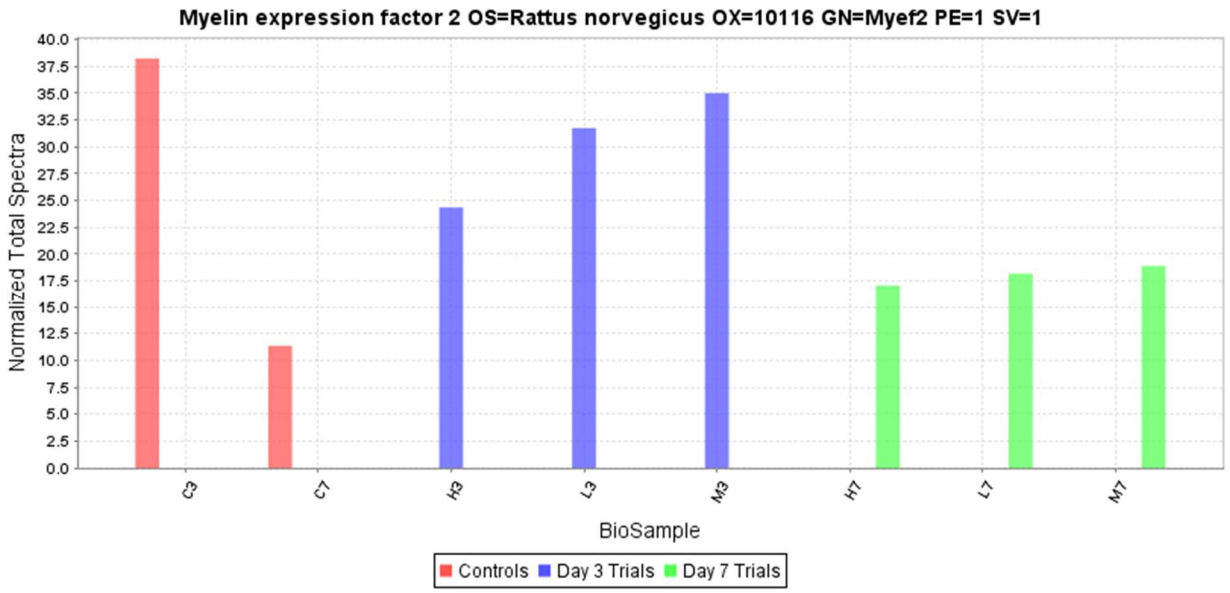

Figure 8. Normalized total spectra of myelin expression factor 2 in the analyzed samples. This data was not deemed statistically significant by the ANOVA test, but was still worth looking at as it could present a lead for future studies.

Post-Translational Modifications

Post-translational modifications (PTMs) have always been a talking point when it comes to histones. Since many different studies have addressed specific PTMs, it was important to analyze the possible PTMs that were found in our samples to see if the affected charge and structure in the peptide sequence would affect histone binding and function. Using a different program now in the form of Peaks Studio X, we compared our samples using a similar algorithm. In this software; however, we were capable of visualizing the proper PTMs at certain sites within the amino acid sequences of each peptide. When comparing the controls to the trials, multiple amino acid sequences were found to be linked with the histone peptides. Some of these

sequences had PTMs that would occur more often than others. For example, when the five Histone H1 variants were processed, four of them showed sequences that were acetylated at the first serine in the amino acid chain (Figure 9). This does not mean that all of these peptides were acetylated, but it does show that some were. Further comprehension of Figure 9 shows that there were other modifications such as carbamylation and ubiquitination. There was little PTM variation seen between the histones for the first 65 amino acids with Histone H1.1 and Histone H1.5 being the most different. De novo peptides were fully matched and the confident modification sites were shown with a minimal ion intensity of 5%. This means that a pair of major fragment ions (b and y ions) must be found showing fragmentation before and after the modified amino acid with at least the given minimum intensity of 5%.

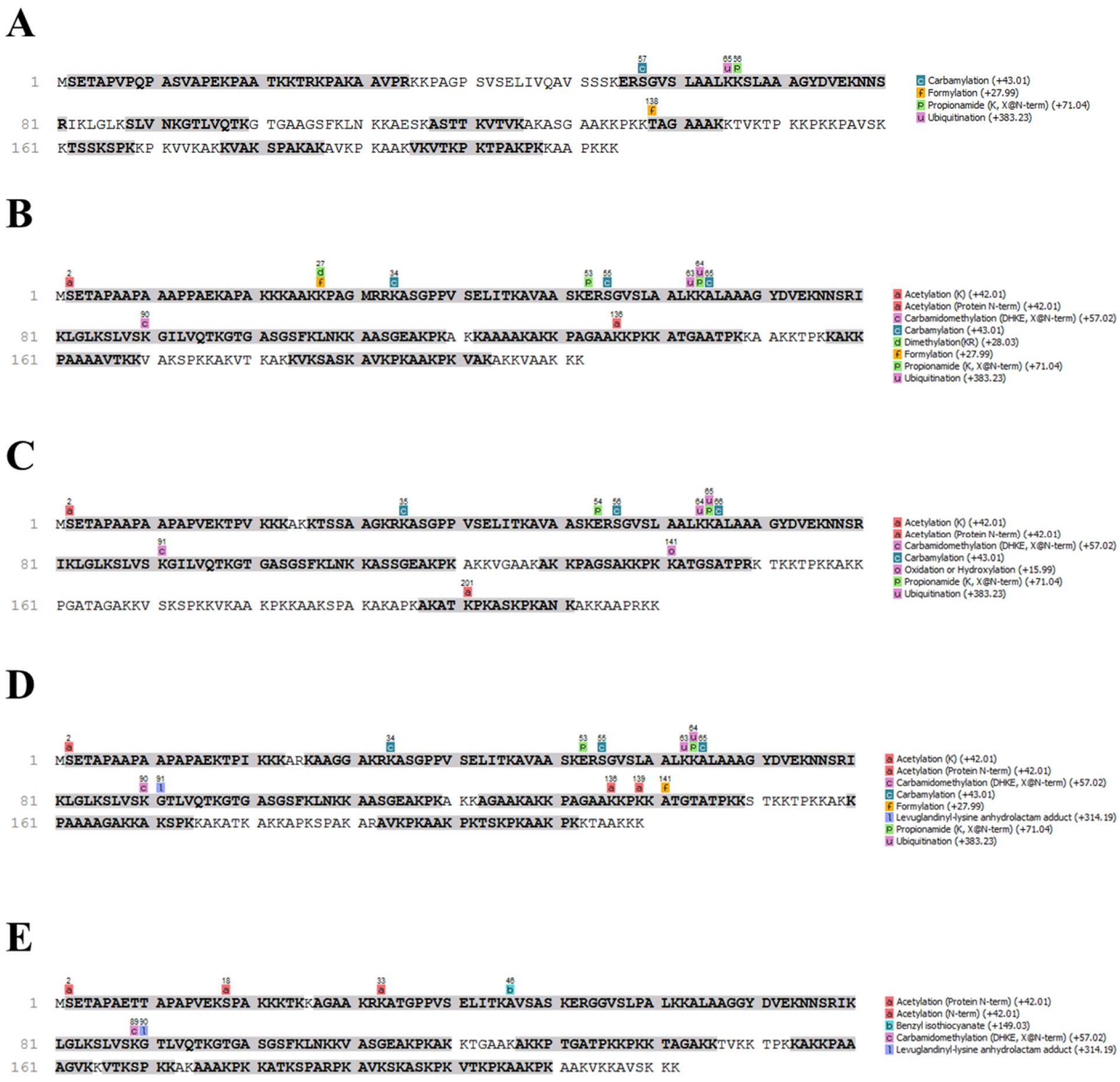

Figure 9. Amino acid sequences of the five variants of histone H1 with possible PTMs labeled at certain sites. Not all copies of these peptides are modified, but there are some that were modified in the samples. A: Histone H1.1. B: Histone cluster 1 family member C. C: Histone cluster 1 family member D. D: Histone H1.4. E: Histone H1.5. Little variation is illustrated between B, C, and D for the first 65 amino acids. Histone H1.1 and Histone H1.5 peptides were capable of being modified a bit differently.

RT-qPCR Analysis

Before the RT-qPCR analysis was conducted, the prepared RNA of every sample was measured for purity by calculating absorbance values through use of the NanoDrop™ 2000c Spectrophotometer (Thermo Scientific™). These values are illustrated below in Table 5.

Table 5
RNA Absorbance Values

Sample	Concentration (µg/µL)	A260/A280	A260/A230
C3	1.9282	1.78	2.21
L3	1.2177	1.75	2.25
M3	0.8436	1.78	2.24
H3	1.2680	1.86	2.08
C7	1.1582	1.80	2.23
L7	1.1262	1.81	2.20
M7	1.0629	1.81	2.09
H7	1.3195	1.84	2.01

Since the samples were confirmed to be pure enough by this data, the RT-qPCR analysis carried on with the use of a continuous fluorescence detector. This machine generated curves that illustrated the relative fluorescence as the cycles carried on. Forty cycles were completed according to the standard PCR specifications listed in the user guide (MAN0013511). After the curves were generated, a cycle time threshold of 0.180 was set to compare how quickly the contents amplified between the different histone H1 variants. Most of the variants exhibited the same basic trend where the curves of the treated groups would cross the threshold sooner than the curves of the control groups for both time points. The (c)T values (cycle time values) were

typically lower for the treatment groups and a bit higher for the control groups, illustrating that generally there was more histone H1 variant RNA in the cells post-treatment with *H .erinaceus* as shown in Figure 10.

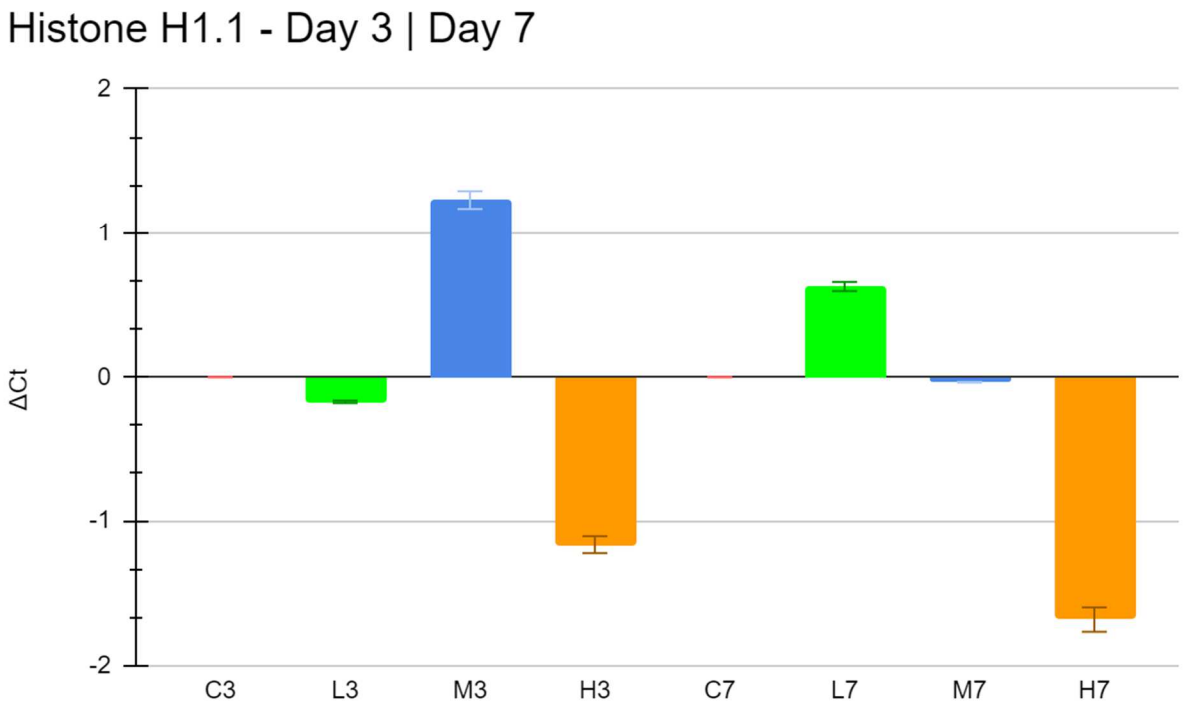
Histone H1.1 - Day 3 | Day 7
ΔCt
2
1
0
-1
-2
C3
L3
M3
H3
C7
L7
M7
H7

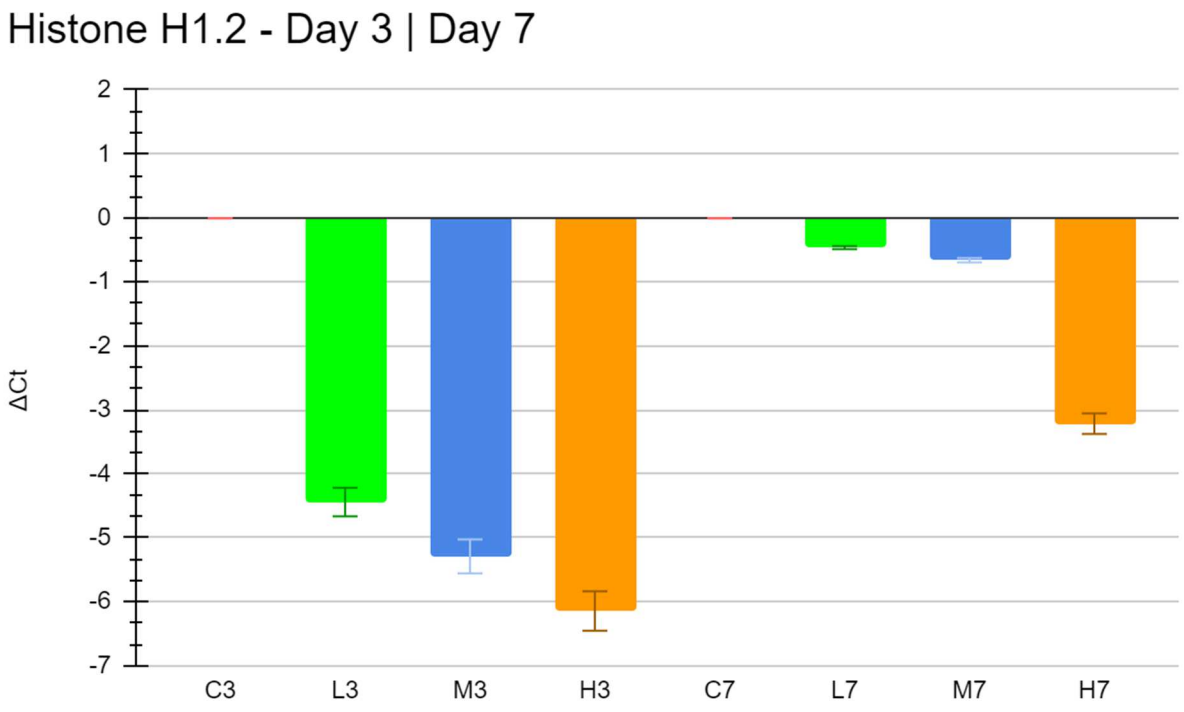
Histone H1.2 - Day 3 | Day 7
ΔCt
2
1
0
-1
-2
-3
-4
-5
-6
-7
C3
L3
M3
H3
C7
L7
M7
H7

(Figure 10 Continued)

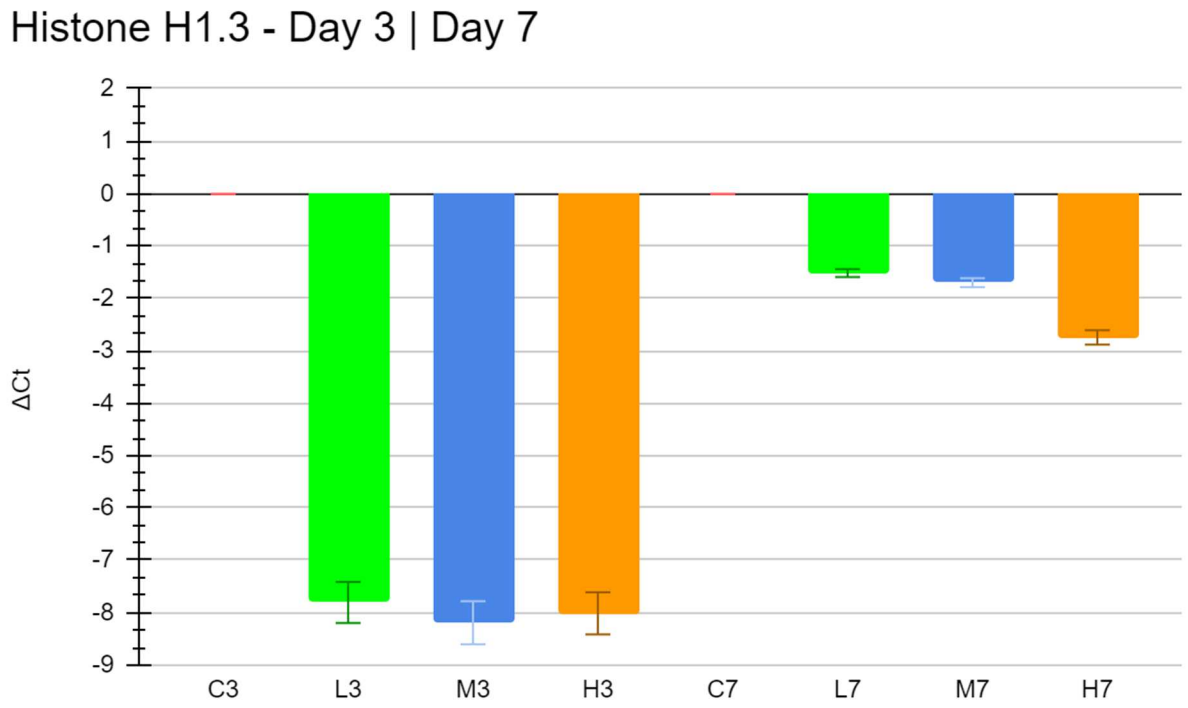

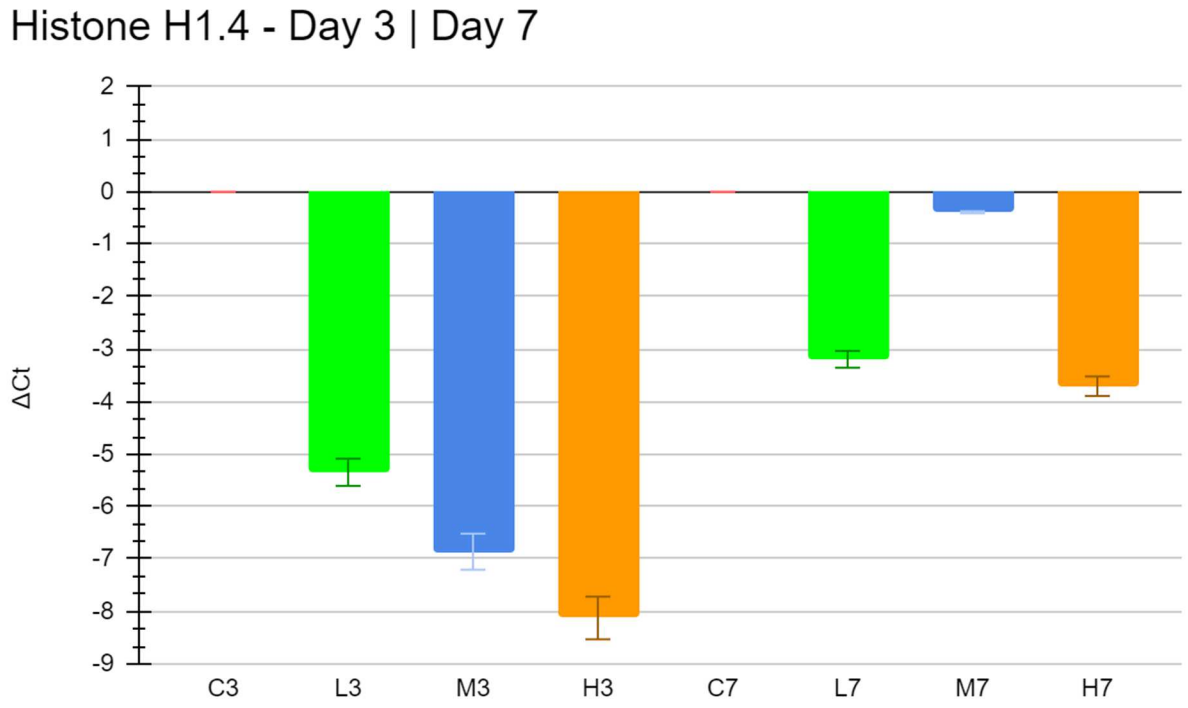

(Figure 10 Continued)

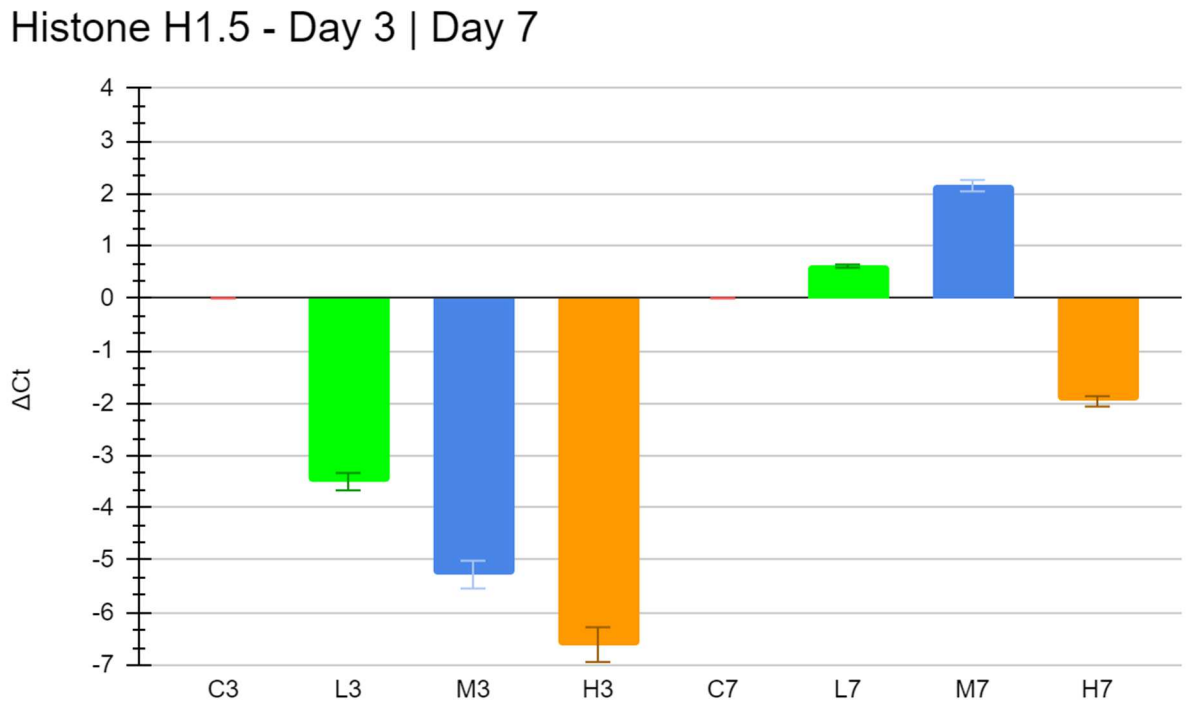

Figure 10. The difference in cycle time compared across the histone H1 variants. The equation is ΔCt = Cycle time of Trial - Cycle time of Control. The day 3 trials were compared to the day 3 control and the day 7 trials were compared to the day 7 control. The threshold of 0.180 was crossed during the RT-qPCR analysis of each sample for every histone H1 variant. Both time points are illustrated in each graph. The more negative differences indicate more initial RNA in the sample for the depicted histone H1 variant as compared to the more positive differences which indicate less. Similar trends are visualized across all histone H1 variants analyzed.

CHAPTER 4: DISCUSSION

Neural Stem Cell Differentiation

Nervous tissue is notorious for being very delicate and although we performed every step meticulously, there was always a chance for contamination or inefficient growth. We kept this in mind as the results were processed. We initially wanted to treat the neural stem cells with larger concentrations of *H. erinaceus* extract to rival studies published previously; however, this proved to be difficult as the *H. erinaceus* extract powder failed to completely dissolve when added to the incomplete medium. After decreasing the concentrations through multiple iterations, the strongest concentration that could be completely dissolved in the medium (defined by no particles visible) was set to 0.5 mg/mL. The other two weaker concentrations were chosen for relative ease of calculation. After confirming that there were no particles to be seen in the mixture following addition of the powder, the mixtures were poured over a microfilter as another safety measure to ensure no contamination during the mixing process. Unfortunately, some of the material that was filtered out of the solution seemed to be particles of *H. erinaceus*. We were not able to measure the exact amount that did not pass through the microfilter and we did not know how this would affect our results. We were unable to restart the procedure as the cells were already in the process of growing and our supply of media was running low. It would have been ideal to run this experiment once more using different conditions, but due to financial and time restraints, we were limited to this path that we already started on. Despite this hiccup, we decided to continue with the experiment as it was. When observing the morphology of the differentiated cells under the electron microscope, little variation between the different concentrations of treatment groups was seen within the same day of trials. The data analyzed

during the later stages of the proteomic analysis reinforces the lack of variation except for when it came to the dense clustering of the cells seen in the Low Day 7 trials. The medium and high concentration counterparts did not exhibit such specific clustering and showed a broader distribution of cells with less clusters. According to these signs, one would assume that these higher concentrations are affecting the differentiation in an impactful way. However, even with the unique clusters seen in the Low Day 7 trials, the proteomic data bolsters the fact that this interesting morphology does not significantly impact the expression of proteins. It is unclear if this is due to insufficient concentration of *H. erinaceus* affecting the cells or if more time has to pass to visualize these differences more distinctly. It may also be possible that *H. erinaceus* has no effect whatsoever on the morphology of the cells and that it may only affect gene and protein expression unrelated to external physical appearance.

Normalization and Mass Spectrometry

Prior to running our samples through the mass spectrometer, we decided to lyophilize the samples in order to increase the concentration of protein. This allows the mass spectrometer to register more effective scans. During the colorimetric peptide assay, peptide concentration was recorded; however, one of the two biological replicates of each sample was more concentrated than the other and was chosen to be used for the mass spectrometry. Using the sample with the lowest concentration of total peptides (3C2), we normalized the other samples so the total peptide concentration would be closely similar across the board (Table 3). This was important to maintain consistency during the experiment. Randomizing the order of the samples during the run was key in preventing the occurrence of unwanted bias and variables. The samples were double-injected in order to create technical replicates. The technical replicates of the samples were also randomized and did not go in the same order as the original samples. A sample of

HeLa cells was injected multiple times in equal time intervals in between our samples to provide evidence for the machine's consistency in spray pattern. In essence, this functioned as a technical control to see if there were any issues with the mass spectrometer's run itself. No significant variation in spray pattern pattern was found, illustrating that the machine executed the procedure without issues. The mass spectrometer generated chromatographs (Figure 3) that were used to validate our data and vet it before moving on with the software-based quantitative proteomic analysis. The technical replicates generated identical chromatographs as those shown in Figure 3 and were not listed to avoid redundancy.

Quantitative Proteomic Analysis

To ensure a False Discovery Rate (FDR) of less than 0.1%, certain parameters had to be set during the Scaffold analysis. After setting the thresholds to the defined values mentioned in the Results section, we were able to achieve a point where we could analyze every peptide with extremely high confidence. For measuring protein abundance, spectral counting is one of the most effective methods to use. There is a very strong correlation between protein abundance and spectral counts[30]. While another method of protein quantification, measuring ion peak intensity, is available for use, it typically has practical constraints when used for complex biological samples[31]. Because of this, we used spectral counting for our analysis. However, it was vital to normalize the spectral counts in order to measure the variation between samples accurately. The Scaffold program normalized protein spectrum counts by completing multiple calculations in a stepwise manner. First, the total number of spectra in each biosample was calculated. Then, the average number of spectra across all biosamples was calculated. Finally, the spectral count of each protein in every sample was multiplied by the average count over the biosample's total spectral count. An example of this calculation is illustrated by Table 6.

Table 6
Example of Spectral Count Normalization in Scaffold

Biosample A	**Spectral Count**	**Biosample B**	**Spectral Count**	
Protein 1	12	Protein 1	8	
Protein 2	6	Protein 2	3	
Protein 3	4	Protein 3	3	
Total	22	Total	14	Total Average: 18
Biosample A	**Normalized**	**Biosample B**	**Normalized**	
Protein 1	10	Protein 1	10	
Protein 2	5	Protein 2	4	
Protein 3	3	Protein 3	4	

Note. Biosample A protein spectral counts are multiplied by 18/22. Biosample B protein spectral counts are multiplied by 18/14.

The histones illustrated in Figure 6 had overall high normalized spectral counts. Pairing this information with the significance resulting from the statistical analysis, these peptides made for our best targets in the final stages of our research. It seems as though these linker histones could play a role in neural stem cell differentiation. Histone H1 is the most variable of the histones and has multiple variants as seen in this study, but it also has strongly conserved regions which could explain the similar function between the variants[32]. If one Histone H1 variant is being expressed at lower amounts, other variants show a compensatory increase in expression controlled by an unknown mechanism[33]. However, if enough H1 subtypes are lost, embryonic stem cell differentiation is impaired and the silencing of pluripotency factors during DNA methylation mediation is interrupted. This shows that modulating the levels of these linker histones and chromatin compaction may help in regulating stem cell pluripotency[34]. Based on this information from previous studies, we initially believed that the increase in Histone H1

protein expression that is witnessed in Figure 6 correlated to an increase in embryonic stem cell differentiation and was resulting in a faster differentiation process. To verify this, we sought out potential downstream targets that might be regulated by these changes in the histones. These targets were markers that were previously discussed in other studies relating to the nervous system and differentiation. If our initial theory was correct, then the markers for increased differentiation should increase in expression. Lower levels would be illustrated in the control groups and higher levels would be illustrated in the treated samples. We examined standard markers such as neuron-specific enolase (for neuron growth) and glial fibrillary acidic protein (for glial growth), but the results did not support our theory. Levels of these markers were actually higher in the control group, demonstrating that differentiation was not occurring at a faster rate in the treatment groups since neuronal and glial synthesis was not accelerating according to these keystone markers. There is still room for improvement on this end as not even a major proteomic marker of myelin sheath synthesis, MBP, was found during the proteomic analysis. Considering that it is capable of being found by mass spectrometry[37], our protocol could be refined to better isolate this protein from within the lipid membrane of myelin[38]. The lack of this protein in the analyzed sample is odd considering that the transcriptional repressor for it was found and changes in protein expression levels were seen as the days passed. This may be due to the time limits implemented during this study being too short and the protein itself not forming in enough abundance yet. Although there was glial growth as illustrated by the darker spots during light microscopy, perhaps not enough mature oligodendrocyte formation occurred.

Post-Translational Modifications

Another software, Peaks Studio X (Proteome Software, Inc.™) was used to confirm the data found in Scaffold. Peaks Studio X uses a slightly different algorithm to calculate the False Discovery Rate and other metrics; however, all the results still pointed towards the previously discussed histones. More importantly, this software allowed us to analyze the effect of post-translational modifications on the Histone H1 family. It is known that Histone H1 variants are filled with many lysine and arginine residues and are therefore positively charged. This strong positive charge will allow for tight binding to DNA during chromatin compaction. These linker histones can act as transcriptional repressors or promoters when this binding occurs. However, more studies link these histones to the function of local repression[35]. Post translational modifications such as methylation and acetylation make it more difficult for these linker histones to tightly bind to the wound chromatin due to the decrease in positive charge and the structural change of the histones. These changes particularly impact the terminal parts of the protein sequence which are thought to be involved in binding of chromatin proteins regulating transcriptional activity[36]. Our results are illustrated in Figure 9, showing post-translational modifications that have occurred at certain parts in the sequence for a certain number of Histone H1 peptides. Not all H1 peptides experienced post-translational modifications, but the ones that did experienced them in various regions. The most similar ones being Histone H1.2 (family member C), H1.3 (family member D), and H1.4 with a lysine residue at position 64 and/or 65 experiencing ubiquitination. Histone H1.1 is most likely experiencing significantly different modifications because it is considered a specific variant for thymus, testis, spleen, lymphocytic, and neuronal cells[36]. Although the Histone H1 proteins act as regulators of individual gene transcription through chromatin remodeling, nucleosome spacing, and DNA methylation, not

much methylation was witnessed in our data. The charge of the proteins would remain overwhelmingly positive and there would not be a large enough shift in molecular structure seen to affect the tight binding of these linker histones significantly. Still, this is worth exploring in the future to calculate the actual difference in binding between modified histones and non-modified histones.

Conclusion and Future Directions

This exploratory research should serve as a gateway for future projects in the field of proteomics, *H. erinaceus,* and alternative medicine. There are still many unknowns about the pathways within the nervous system and how it is affected when treated with *H. erinaceus*. Based on previous studies, it is clear that there are benefits to consuming this mushroom, but to what extent these treatments provide benefits is still left to be seen. The relationship between the histones observed in this study and the fungal extract provides a small, yet novel benefit to the differentiation process in stem cells. With protocol refinement, *H. erinaceus* might be used in the future as a supplement to growth media when differentiating cells.

It is worth noting that we did have limitations that future studies can avoid when attempting to build upon this one. To our knowledge, we were the first to attempt a quantitative and label-free proteomic analysis on rat neural stem cells after being treated with aqueous extract of *H. erinaceus*. We did not find any previous studies that covered this exact topic; therefore, we did not have a specific guide on how to proceed flawlessly. We were forced to pull information from many facets of the groups currently analyzing *H. erinaceus* and its effects. We were also limited due to the sensitive nature of the neural stem cells. We would have preferred to work with human tissue to analyze the medicinal benefits in a better way, but due to costs, our lab was limited to animal cells such as those from rats. These cells were cultured from a primary cell line

and, as a result, were very difficult to work with. Having an immortal cell line would allow us more time and resources and we would not have to worry about running out of products. It would have been less expensive and would have also allowed us to run the procedure for a longer period of time to witness the effects on a deeper level. Running the experiment again for a longer period of time would be very useful in specifically seeing if MBP was indeed in the sample, but did not have enough time to build up to significant protein levels. Previously successful studies have demonstrated progress when utilizing nerve growth factor in their experiments involving neural stem cells[19].

Although having a larger group working on analyzing and researching every protein in our data would have allowed us to deliver more insight on this topic, the results presented in this paper are of the best quality that was allowed due to our restrictions. We are confident that this is a good first step through the door and that others will find this information helpful when proceeding with more sharpened procedures for analyzing the proteomic contents of rat neural tissue post-treatment with *H. erinaceus* extract.

REFERENCES

1. Aydinli F.İ., Çelik E., Vatandaşlar B.K., Kerman, B. E. Myelin disorders and stem cells: as therapies and models. *Turk. J. Biol,* **2016**, *40,* 1068-1080.
2. Leray E., Moreau T., Fromont A., Edan G. Epidemiology of multiple sclerosis. *Rev Neurol (Paris)*. **2015**, *172(1),* 3–13.
3. Xinke Z., Joel H., Xiaoli N. Cost Effectiveness of Fingolimod, Teriflunomide, Dimethyl Fumarate and Intramuscular Interferon-β in Relapsing-Remitting Multiple Sclerosis. *CNS Drugs.* **2015**, *29(1),* 71-81.
4. Zhang C., Cao C., Kubo M., Harada K., Yan X., Fukuyama Y., Gao J. Chemical Constituents from Hericium erinaceus Promote Neuronal Survival and Potentiate Neurite Outgrowth via the TrkA/Erk1/2 Pathway. **2017**, *18(8),* 1659- 1672.
5. Di, Lu. Ancient Chinese people's knowledge of macrofungi during the period from 220 to 589. *East Asian Science, Technology & Medicine.* **2014**, *37*, 36-68.
6. Jiang, S.; Wang, S.; Sun, Y.; Zhang, Q. Medicinal properties of Hericium erinaceus and its potential to formulate novel mushroom-based pharmaceuticals. *Applied Microbiology and Biotechnology.* **2014**, *98(18)*, 7661–7670.
7. Blaser M.J. Who are we? Indigenous microbes and the ecology of human diseases. *EMBO Rep.* **2006**, *7(10),* 956–960.
8. Shang X., Tan Q., Liu R., Yu K, Li P., Zhao G.P. In vitro anti-Helicobacter pylori effects of medicinal mushroom extracts, with special emphasis on the Lion's Mane mushroom, Hericium erinaceus (higher Basidiomycetes). *Int. J. Med. Mushrooms.* **2013**, *15(2),* 165–174.
9. Yang B.K., Park J.B., Song C.H. Hypolipidemic effect of exopolymer produced in submerged mycelial culture of five different mushrooms. *J. Microbiol. Biotechnol.* **2002**, *12(6),* 957–961.
10. Yang B.K., Park J.B., Song C.H. Hypolipidemic effect of an exobiopolymer produced from a submerged mycelial culture of Hericium erinaceus. *Biosci. Biotechnol. Biochem.* **2003**, *67(6),* 1292–1298.
11. Wong K.H., Naidu M., David P., Abdulla M.A., Abdullah N., Kuppusamy U.R., Sabaratnam V. Peripheral nerve regeneration following crush injury to rat peroneal nerve by aqueous extract of medicinal mushroom Hericium erinaceus (Bull.: Fr) Pers. (Aphyllophoromycetideae). *Evidence Based Complementary and Alternative Medicine.* **2011**, *2011,* 1-10.
12. Moldavan M.G., Gryganski A.P., Kolotushkina O.V., Kirchhoff B., Skibo G.G., Pedarzani P. Neurotropic and trophic action of lion's mane mushroom Hericium erinaceus (Bull.: Fr.) Pers. (Aphyllophoromycetideae) extracts on nerve cells in vitro. *Int. J. Med. Mushrooms.* **2007**, *9*, 15–28.
13. Lee E.W., Shizuki K., Hosokawa S., Suzuki M., Suganuma H., Inakuma T., Li J., Ohnishi-Kameyama M., Nagata T., Furukawa S., Kawagishi H. Two Novel Diterpenoids,

Erinacines H and I from the Mycelia of *Hericium erinaceum*. *Bioscience, Biotechnology, and Biochemistry*. **2000**, *64(11)*, 2402-2405.

14. Kolotushkina E.V., Moldavan M.G., Voronin K.Y., Skibo G.G. The influence of Hericium erinaceus extract on myelination process in vitro. *Fiziol. Zh.* **2003**, *49(1),* 38–45.
15. Compston A., Coles A. Multiple Sclerosis. *The Lancet.* **2008**, *372(9648)*, 1502-1517.
16. Kim Y., Krause T. M., Blum P., Freeman L. Disease modifying therapies continue to drive up health care cost among individuals with multiple sclerosis. **2019**, *30*, 69-75.
17. Sorensen P.S. Multiple sclerosis: pathophysiology revisited. *The Lancet Neurology*. **2005**, *4(1)*, 9-10.
18. Ksiazek-Winiarek D.J., Szpakowski P., Glabinski A. Neural Plasticity in Multiple Sclerosis: The Functional and Molecular Background. *Neural Plasticity*. **2015**, *2015*, 1-11.
19. Wang Q., Song Y. H., Tang Z., Wang Z. P., Xu Q., Bao N. Effects of ganglioside GM1 and neural growth factor on neural stem cell proliferation and differentiation. *Genetics and Molecular Research*. **2016**, *15(3)*, 1-9.
20. Wang M., Kanako N., Zhang Y., Xiao X., Gao Q., Tetsuya K. A unique polysaccharide purified from *Hericium erinaceus* mycelium prevents oxidative stress induced by H_2O_2 in human gastric mucosa epithelium cell. *PLoS ONE*. **2017**, 12(7), 1-14.
21. Friedman, M. Chemistry, Nutrition, and Health-Promoting Properties of *Hericium erinaceus* (Lion's Mane) Mushroom Fruiting Bodies and Mycelia and Their Bioactive Compounds. *J. Agric. Food Chem.* **2015**, 63(32), 7108-7123.
22. Baldassari L. E., Feng J., Clayton B. L. L., Oh S., Sakaie K., Tesar P. J., Wang Y., Cohen J. A. Developing therapeutic strategies to promote myelin repair in multiple sclerosis. *Expert Review of Neurotherapeutics*. **2019**, 19(10), 997-1013.
23. Mori K., Obara Y., Hirota M., Azumi Y., Kinugasa S., Inatomi S., Nakahata N. Nerve Growth Factor-Inducing Activity of *Hericium erinaceus* in 1321N1 Human Astrocytoma Cells. *Biol. Pharm. Bull.* **2008**, 31(9), 1727-1732.
24. Li I., Lee L., Tzeng T., Chen W., Chen Y., Shiao Y., Chen C. Neurohealth Properties of *Hericium erinaceus* Mycelia Enriched with Erinacines. *Behavioural Neurology*. **2018**, 2018, 1-10.
25. Wu F., Zhou C., Zhou D., Ou S., Zhang X., Huang H. Structure characterization of a novel polysaccharide from *Hericium erinaceus* fruiting bodies and its immunomodulatory activities. *Food Funct.* **2018**, 9, 294-306.
26. Zeng X., Ling H., Yang J., Chen J., Guo S. Proteome analysis provides insight into the regulation of bioactive metabolites in *Hericium erinaceus*. *Gene*. **2018**, 666, 108-115.
27. Hebert A., Richards A., Bailey D., Ulbrich A., Coughlin E., Westphall M., Coon J. The One Hour Yeast Proteome. *Mol Cell Proteomics.* **2014**, 13(1), 339-347.

28. Park D., Xiang A. P., Mao F. F., Zhang L., Di C., Liu X., Shao Y., Ma B., Lee J., Ha K., Walton N., Lahn B. T. Nestin Is Required for the Proper Self-Renewal of Neural Stem Cells. *Stem Cells.* **2010**, 28(12), 2162-2171.
29. Steplewski A, Haas S, Amini S, Khalili K. Regulation of mouse myelin basic protein gene transcription by a sequence-specific single-stranded DNA-binding protein in vitro. *Gene*. **1995**, 154(2), 215-218.
30. Lundgren D., Hwang S., Wu L., Han D. Role of spectral counting in quantitative proteomics. *Expert Review of Proteomics*. **2010**, 7(1), 39-53.
31. Zhu W., Smith J., Huang C. Mass Spectrometry-Based Label-Free Quantitative Proteomics. *BioMed Research International*. **2009**, 2010, 1-6.
32. Isenberg, I. Histones. *Ann. Rev. Biochem.* **1979**, 48, 159-191.
33. Pan C., Fan Y. Role of H1 linker histones in mammalian development and stem cell differentiation. *Biochimica et Biophysica Acta.* **2016**, 1859. 496-509.
34. Zhang Y., Cooke M., Panjwani S., Cao K., Krauth B., Ho P., Medrzycki M., Berhe D., Pan C., McDevitt T., Fan Y. Histone H1 Depletion Impairs Embryonic Stem Cell Differentiation. *PLoS Gene*. **2012**, 8(5), 1-14.
35. Kuzmichev A., Jenuwein T., Tempst P., Reinberg D. Different EZH2-containing complexes target methylation of histone H1 or nucleosomal histone H3. *Mol. Cell.* **2004**, 14, 183-193.
36. Wisniewski J., Zougman A., Kruger S., Mann M. Mass Spectrometric Mapping of Linker Histone H1 Variants Reveals Multiple Acetylations, Methylations, and Phosphorylation as Well as Differences between Cell Culture and Tissue. *Molecular & Cellular Proteomics*. **2007**, 6(1), 72-87.
37. Plymire D., Wing C., Robinson D., Patrie S. Continuous Elution Proteoform Identification of Myelin Basic Protein by Superficially Porous Reversed-Phase Liquid Chromatography and Fourier Transform Mass Spectrometry. *Anal. Chem.* **2017**, 89(22), 12030-12038.
38. Rispoli P., Carzino R., Svaldo-Lanero T., Relini A., Cavalleri O., Fasano A., Liuzzi G., Carlone G., Riccio P., Gliozzi A., Rolandi R. A Thermodynamic and Structural Study of Myelin Basic Protein in Lipid Membrane Models. *Biophysical Journal.* **2007**, 93, 1999-2010.

APPENDIX A: LIST OF T-TEST SIGNIFICANT PROTEINS AND FOLD CHANGES IN DAY 3 GROUPS

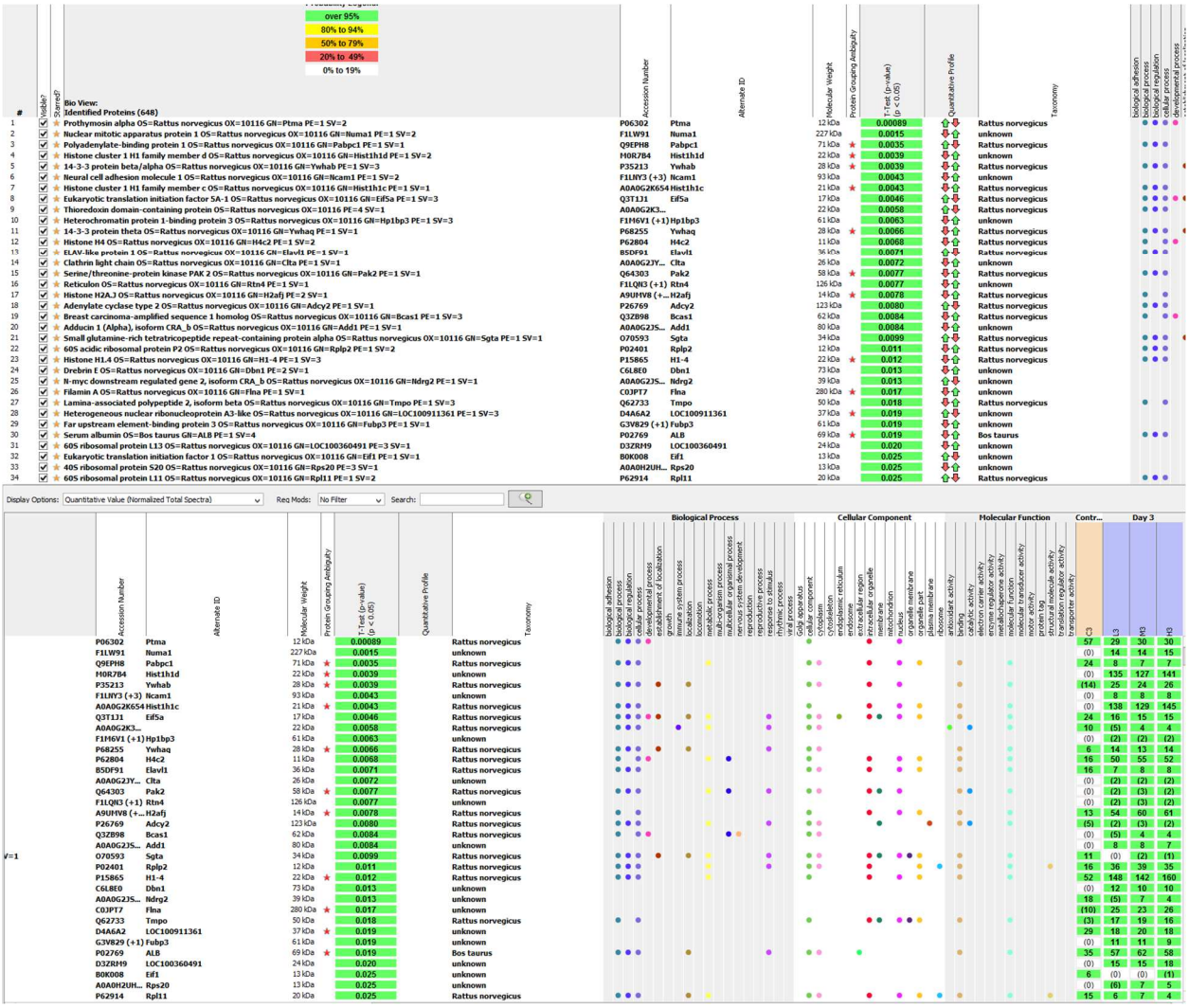

#	Bio View: Identified Proteins (648)	Accession Number	Alternate ID	Molecular Weight	Protein Grouping Ambiguity	T-Test (p-value) (p < 0.05)	Quantitative Profile	Taxonomy	C3	L3	M3	H3
1	Prothymosin alpha OS=Rattus norvegicus OX=10116 GN=Ptma PE=1 SV=2	P06302	Ptma	12 kDa		0.00089		Rattus norvegicus	57	29	30	30
2	Nuclear mitotic apparatus protein 1 OS=Rattus norvegicus OX=10116 GN=Numa1 PE=1 SV=2	F1LW91	Numa1	227 kDa		0.0015		unknown	(0)	14	14	15
3	Polyadenylate-binding protein 1 OS=Rattus norvegicus OX=10116 GN=Pabpc1 PE=1 SV=1	Q9EPH8	Pabpc1	71 kDa	*	0.0035		Rattus norvegicus	24	8	7	7
4	Histone cluster 1 H1 family member d OS=Rattus norvegicus OX=10116 GN=Hist1h1d PE=1 SV=2	M0R7B4	Hist1h1d	22 kDa	*	0.0039		unknown	(0)	135	127	141
5	14-3-3 protein beta/alpha OS=Rattus norvegicus OX=10116 GN=Ywhab PE=1 SV=3	P35213	Ywhab	28 kDa	*	0.0039		Rattus norvegicus	(14)	25	24	26
6	Neural cell adhesion molecule 1 OS=Rattus norvegicus OX=10116 GN=Ncam1 PE=1 SV=2	F1LNY3 (+3)	Ncam1	93 kDa		0.0043		unknown	(0)	8	8	8
7	Histone cluster 1 H1 family member c OS=Rattus norvegicus OX=10116 GN=Hist1h1c PE=1 SV=1	A0A0G2K654	Hist1h1c	21 kDa	*	0.0043		Rattus norvegicus	(0)	138	129	145
8	Eukaryotic translation initiation factor 5A-1 OS=Rattus norvegicus OX=10116 GN=Eif5a PE=1 SV=3	Q3T121	Eif5a	17 kDa		0.0046		Rattus norvegicus	24	16	15	15
9	Thioredoxin domain-containing protein OS=Rattus norvegicus OX=10116 PE=4 SV=1	A0A0G2K3...		22 kDa		0.0058		Rattus norvegicus	10	(5)	4	4
10	Heterochromatin protein 1-binding protein 3 OS=Rattus norvegicus OX=10116 GN=Hp1bp3 PE=1 SV=3	F1M6V1 (+1)	Hp1bp3	61 kDa		0.0063		unknown	(0)	(2)	(2)	(2)
11	14-3-3 protein theta OS=Rattus norvegicus OX=10116 GN=Ywhaq PE=1 SV=1	P68255	Ywhaq	28 kDa	*	0.0066		Rattus norvegicus	6	14	13	14
12	Histone H4 OS=Rattus norvegicus OX=10116 GN=H4c2 PE=1 SV=2	P62804	H4c2	11 kDa		0.0068		Rattus norvegicus	16	50	55	52
13	ELAV-like protein 1 OS=Rattus norvegicus OX=10116 GN=Elavl1 PE=1 SV=1	B5DF91	Elavl1	36 kDa		0.0071		Rattus norvegicus	16	7	8	8
14	Clathrin light chain OS=Rattus norvegicus OX=10116 GN=Clta PE=1 SV=1	A0A0G2JY...	Clta	26 kDa		0.0072		unknown	(0)	(2)	(2)	(2)
15	Serine/threonine-protein kinase PAK 2 OS=Rattus norvegicus OX=10116 GN=Pak2 PE=1 SV=1	Q64303	Pak2	58 kDa	*	0.0077		Rattus norvegicus	(0)	(2)	(3)	(2)
16	Reticulon OS=Rattus norvegicus OX=10116 GN=Rtn4 PE=1 SV=1	F1LQN3 (+1)	Rtn4	126 kDa		0.0077		unknown	(0)	(2)	(3)	(2)
17	Histone H2A.J OS=Rattus norvegicus OX=10116 GN=H2afj PE=2 SV=1	A9UHV8 (+...	H2afj	14 kDa	*	0.0078		Rattus norvegicus	13	54	60	61
18	Adenylate cyclase type 2 OS=Rattus norvegicus OX=10116 GN=Adcy2 PE=1 SV=1	P26769	Adcy2	123 kDa		0.0080		Rattus norvegicus	(5)	(2)	(3)	(2)
19	Breast carcinoma-amplified sequence 1 homolog OS=Rattus norvegicus OX=10116 GN=Bcas1 PE=1 SV=3	Q3ZB98	Bcas1	62 kDa		0.0084		Rattus norvegicus	(0)	(5)	4	4
20	Adducin 1 (Alpha), isoform CRA_b OS=Rattus norvegicus OX=10116 GN=Add1 PE=1 SV=1	A0A0G2JS...	Add1	80 kDa		0.0084		unknown	(0)	8	8	7
21	Small glutamine-rich tetratricopeptide repeat-containing protein alpha OS=Rattus norvegicus OX=10116 GN=Sgta PE=1 SV=1	O70593	Sgta	34 kDa		0.0099		Rattus norvegicus	11	(0)	(2)	(1)
22	60S acidic ribosomal protein P2 OS=Rattus norvegicus OX=10116 GN=Rplp2 PE=1 SV=2	P02401	Rplp2	12 kDa		0.011		Rattus norvegicus	16	36	39	35
23	Histone H1.4 OS=Rattus norvegicus OX=10116 GN=H1-4 PE=1 SV=3	P15865	H1-4	22 kDa	*	0.012		Rattus norvegicus	52	148	142	160
24	Drebrin E OS=Rattus norvegicus OX=10116 GN=Dbn1 PE=2 SV=1	C6L8E0	Dbn1	73 kDa		0.013		unknown	(0)	12	10	10
25	N-myc downstream regulated gene 2, isoform CRA_b OS=Rattus norvegicus OX=10116 GN=Ndrg2 PE=1 SV=1	A0A0G2JS...	Ndrg2	39 kDa		0.013		unknown	18	(5)	7	4
26	Filamin A OS=Rattus norvegicus OX=10116 GN=Flna PE=1 SV=1	C0JPT7	Flna	280 kDa	*	0.017		unknown	(10)	25	23	26
27	Lamina-associated polypeptide 2, isoform beta OS=Rattus norvegicus OX=10116 GN=Tmpo PE=1 SV=3	Q62733	Tmpo	50 kDa		0.018		Rattus norvegicus	(3)	17	19	16
28	Heterogeneous nuclear ribonucleoprotein A3-like OS=Rattus norvegicus OX=10116 GN=LOC100911361 PE=1 SV=3	D4A6A2	LOC100911361	37 kDa	*	0.019		unknown	29	18	20	18
29	Far upstream element-binding protein 3 OS=Rattus norvegicus OX=10116 GN=Fubp3 PE=1 SV=1	G3V829 (+1)	Fubp3	61 kDa		0.019		unknown	(0)	11	11	9
30	Serum albumin OS=Bos taurus GN=ALB PE=1 SV=4	P02769	ALB	69 kDa	*	0.019		Bos taurus	35	57	62	58
31	60S ribosomal protein L13 OS=Rattus norvegicus OX=10116 GN=LOC100360491 PE=3 SV=1	D3ZRM9	LOC100360491	24 kDa		0.020		unknown	(0)	15	15	18
32	Eukaryotic translation initiation factor 1 OS=Rattus norvegicus OX=10116 GN=Eif1 PE=1 SV=1	B0K008	Eif1	13 kDa		0.025		unknown	6	(0)	(0)	(1)
33	40S ribosomal protein S20 OS=Rattus norvegicus OX=10116 GN=Rps20 PE=3 SV=1	A0A0H2UH...	Rps20	13 kDa		0.025		unknown	(0)	(6)	7	5
34	60S ribosomal protein L11 OS=Rattus norvegicus OX=10116 GN=Rpl11 PE=1 SV=2	P62914	Rpl11	20 kDa		0.025		Rattus norvegicus	15	6	7	4

35	Vimentin OS=Rattus norvegicus OX=10116 GN=Vim PE=1 SV=2	P31000	Vim	54 kDa	*	0.025		
36	Histone H2B OS=Rattus norvegicus OX=10116 GN=Hist1h2bk PE=3 SV=1	G3V9C7	Hist1h2bk	14 kDa		0.025		
37	T-complex protein 1 subunit beta OS=Rattus norvegicus OX=10116 GN=Cct2 PE=1 SV=3	Q5XIM9	Cct2	57 kDa		0.027		
38	Peptidyl-prolyl cis-trans isomerase FKBP1A OS=Rattus norvegicus OX=10116 GN=Fkbp1a PE=1 SV=3	Q62658	Fkbp1a	12 kDa		0.031		
39	Calmodulin-3 OS=Rattus norvegicus OX=10116 GN=Calm3 PE=1 SV=1	P0DP31	Calm3	17 kDa		0.031		
40	Metastasis-associated protein MTA1 OS=Rattus norvegicus OX=10116 GN=Mta1 PE=1 SV=1	A0A140TA98	Mta1	83 kDa		0.033		
41	Dihydropyrimidinase-related protein 2 OS=Rattus norvegicus OX=10116 GN=Dpysl2 PE=1 SV=1	P47942	Dpysl2	62 kDa	*	0.033		
42	Histone H2B OS=Rattus norvegicus OX=10116 GN=Hist1h2bl PE=3 SV=1	M0R4L7	Hist1h2bl	14 kDa		0.033		
43	Cleavage and polyadenylation specificity factor subunit 5 OS=Rattus norvegicus OX=10116 GN=Nudt21 PE=2 SV=1	B4F764	Nudt21	26 kDa		0.034		
44	RCG55135, isoform CRA_b OS=Rattus norvegicus OX=10116 GN=Tln1 PE=1 SV=1	G3V852	Tln1	270 kDa	*	0.035		
45	Eukaryotic translation initiation factor 4H OS=Rattus norvegicus OX=10116 GN=Eif4h PE=1 SV=1	Q5XI72	Eif4h	27 kDa		0.036		
46	Brain acid soluble protein 1 OS=Rattus norvegicus OX=10116 GN=Basp1 PE=1 SV=2	Q05175	Basp1	22 kDa	*	0.036		
47	Peptidyl-prolyl cis-trans isomerase OS=Rattus norvegicus OX=10116 GN=Pin1 PE=1 SV=1	B0BNL2	Pin1	18 kDa		0.036		
48	10 kDa heat shock protein, mitochondrial OS=Rattus norvegicus OX=10116 GN=Hspe1 PE=1 SV=1	A0A0G2JTG1	Hspe1	9 kDa		0.037		
49	Centromere protein V OS=Rattus norvegicus OX=10116 GN=Cenpv PE=1 SV=3	D4A9A3	Cenpv	28 kDa		0.038		
50	Alpha-enolase OS=Rattus norvegicus OX=10116 GN=Eno1 PE=1 SV=4	P04764 (+1)	Eno1	47 kDa	*	0.038		
51	Matrin-3 OS=Rattus norvegicus OX=10116 GN=Matr3 PE=1 SV=2	P43244	Matr3	94 kDa		0.040		
52	Transient receptor potential cation channel subfamily V member 4 OS=Rattus norvegicus OX=10116 GN=Trpv4 PE=1 SV=1	Q9ERZ8	Trpv4	98 kDa		0.041		
53	ATP synthase membrane subunit DAPIT, mitochondrial OS=Rattus norvegicus OX=10116 GN=Atp5md PE=1 SV=1	Q9JJW3	Atp5md	6 kDa		0.041		
54	Aly/REF export factor OS=Rattus norvegicus OX=10116 GN=Alyref PE=1 SV=1	D3ZXH7	Alyref	20 kDa		0.042		
55	Cytochrome c oxidase subunit 4 isoform 1, mitochondrial OS=Rattus norvegicus OX=10116 GN=Cox4i1 PE=1 SV=1	P10888	Cox4i1	20 kDa		0.042		
56	60S acidic ribosomal protein P1 OS=Rattus norvegicus OX=10116 GN=Rplp1 PE=3 SV=1	P19944	Rplp1	11 kDa		0.043		
57	Isoaspartyl peptidase/L-asparaginase OS=Rattus norvegicus OX=10116 GN=Asrgl1 PE=1 SV=1	Q8VI04	Asrgl1	34 kDa		0.043		
58	Calponin-3 OS=Rattus norvegicus OX=10116 GN=Cnn3 PE=1 SV=1	P37397	Cnn3	36 kDa	*	0.043		
59	Polypyrimidine tract-binding protein 1 OS=Rattus norvegicus OX=10116 GN=Ptbp1 PE=1 SV=1	A0A0G2JTV...	Ptbp1	59 kDa		0.045		
60	Macrophage migration inhibitory factor OS=Rattus norvegicus OX=10116 GN=Mif PE=1 SV=4	P30904	Mif	12 kDa		0.046		
61	EF-hand domain-containing protein D2 OS=Rattus norvegicus OX=10116 GN=Efhd2 PE=1 SV=1	Q4FZY0	Efhd2	27 kDa		0.046		


Display Options: Quantitative Value (Normalized Total Spectra)
Req Mods: No Filter
Search:
Biological Process
Cellular Component
Molecular Function
Contr...
Day 3
Accession Number
Alternate ID
Molecular Weight
Protein Grouping Ambiguity
T-Test (p-value) (p < 0.05)
Quantitative Profile
Taxonomy
C3
L3
M3
H3
P31000 Vim 54 kDa 0.025 Rattus norvegicus 167 75 54 45
G3V9C7 Hist1h2bk 14 kDa 0.025 unknown (104) (55) (62) (67)
Q5XIH9 Cct2 57 kDa 0.027 Rattus norvegicus 11 (2) (2) (0)
Q62658 Fkbp1a 12 kDa 0.031 Rattus norvegicus (0) 10 8 7
P0DP31 Calm3 17 kDa 0.031 Rattus norvegicus 16 (0) (2) (4)
A0A140TA98 Mta1 83 kDa 0.033 unknown 6 (0) (2) (0)
P47942 Dpysl2 62 kDa 0.033 Rattus norvegicus 49 33 28 33
H0K4L7 Hist1h2bl 14 kDa 0.033 unknown 511 278 307 231
B4F764 Nudt21 26 kDa 0.034 unknown (0) (4) (3) 3
G3V852 Tln1 270 kDa 0.035 unknown (0) 6 8 7
Q5XI72 Eif4h 27 kDa 0.036 Rattus norvegicus 18 (4) 7 (2)
Q05175 Basp1 22 kDa 0.036 Rattus norvegicus (0) 24 24 18
B0BNL2 Pin1 18 kDa 0.036 unknown 6 (0) (2) (0)
A0A0G2JTG1 Hspe1 9 kDa 0.037 unknown (0) 13 13 9
D4A9A3 Cenpv 28 kDa 0.038 unknown (0) (2) 3 3
P04764 (+1) Eno1 47 kDa 0.038 Rattus norvegicus 71 43 34 32
P43244 Matr3 94 kDa 0.040 Rattus norvegicus 24 37 34 34
Q9ERZ8 Trpv4 98 kDa 0.041 Rattus norvegicus (6) (2) (3) (2)
Q93JW3 Atp5md 6 kDa 0.041 Rattus norvegicus (0) 7 5 6
D3ZXH7 Alyref 20 kDa 0.042 unknown (0) 6 5 7
P10888 Cox4i1 20 kDa 0.042 Rattus norvegicus 18 12 10 9
P19944 Rplp1 11 kDa 0.043 Rattus norvegicus (0) 13 10 9
Q8VI04 Asrgl1 34 kDa 0.043 Rattus norvegicus (5) (0) (0) (1)
P37397 Cnn3 36 kDa 0.043 Rattus norvegicus 18 12 11 9
A0A0G2JTV... Ptbp1 59 kDa 0.045 unknown (0) 10 13 14
P30904 Mif 12 kDa 0.046 Rattus norvegicus (0) 10 8 7
Q4FZY0 Efhd2 27 kDa 0.046 Rattus norvegicus 8 (2) (0) (0)

APPENDIX B: LIST OF T-TEST SIGNIFICANT PROTEINS AND FOLD CHANGES IN DAY 7 GROUPS

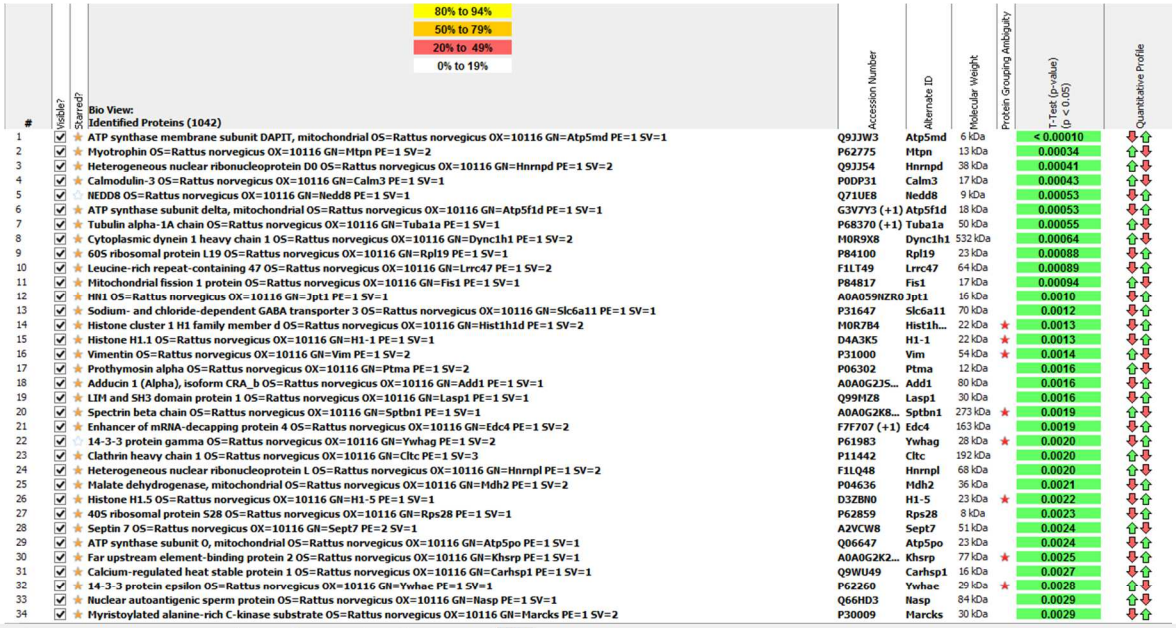

80% to 94%
50% to 79%
20% to 49%
0% to 19%

#	Visible?	Starred?	Bio View: Identified Proteins (1042)	Accession Number	Alternate ID	Molecular Weight	Protein Grouping Ambiguity	T-Test (p-value) (p < 0.05)	Quantitative Profile
1	☑	★	ATP synthase membrane subunit DAPIT, mitochondrial OS=Rattus norvegicus OX=10116 GN=Atp5md PE=1 SV=1	Q9JJW3	Atp5md	6 kDa		< 0.00010	
2	☑	★	Myotrophin OS=Rattus norvegicus OX=10116 GN=Mtpn PE=1 SV=2	P62775	Mtpn	13 kDa		0.00034	
3	☑	★	Heterogeneous nuclear ribonucleoprotein D0 OS=Rattus norvegicus OX=10116 GN=Hnrnpd PE=1 SV=2	Q9JJ54	Hnrnpd	38 kDa		0.00041	
4	☑	★	Calmodulin-3 OS=Rattus norvegicus OX=10116 GN=Calm3 PE=1 SV=1	P0DP31	Calm3	17 kDa		0.00043	
5	☑	☆	NEDD8 OS=Rattus norvegicus OX=10116 GN=Nedd8 PE=1 SV=1	Q71UE8	Nedd8	9 kDa		0.00053	
6	☑	★	ATP synthase subunit delta, mitochondrial OS=Rattus norvegicus OX=10116 GN=Atp5f1d PE=1 SV=1	G3V7Y3 (+1)	Atp5f1d	18 kDa		0.00053	
7	☑	★	Tubulin alpha-1A chain OS=Rattus norvegicus OX=10116 GN=Tuba1a PE=1 SV=1	P68370 (+1)	Tuba1a	50 kDa		0.00055	
8	☑	★	Cytoplasmic dynein 1 heavy chain 1 OS=Rattus norvegicus OX=10116 GN=Dync1h1 PE=1 SV=2	M0R9X8	Dync1h1	532 kDa		0.00064	
9	☑	★	60S ribosomal protein L19 OS=Rattus norvegicus OX=10116 GN=Rpl19 PE=1 SV=1	P84100	Rpl19	23 kDa		0.00088	
10	☑	★	Leucine-rich repeat-containing 47 OS=Rattus norvegicus OX=10116 GN=Lrrc47 PE=1 SV=2	F1LT49	Lrrc47	64 kDa		0.00089	
11	☑	★	Mitochondrial fission 1 protein OS=Rattus norvegicus OX=10116 GN=Fis1 PE=1 SV=1	P84817	Fis1	17 kDa		0.00094	
12	☑	★	HN1 OS=Rattus norvegicus OX=10116 GN=Jpt1 PE=1 SV=1	A0A059NZR0	Jpt1	16 kDa		0.0010	
13	☑	★	Sodium- and chloride-dependent GABA transporter 3 OS=Rattus norvegicus OX=10116 GN=Slc6a11 PE=1 SV=1	P31647	Slc6a11	70 kDa		0.0012	
14	☑	★	Histone cluster 1 H1 family member d OS=Rattus norvegicus OX=10116 GN=Hist1h1d PE=1 SV=2	M0R7B4	Hist1h...	22 kDa	★	0.0013	
15	☑	★	Histone H1.1 OS=Rattus norvegicus OX=10116 GN=H1-1 PE=1 SV=1	D4A3K5	H1-1	22 kDa	★	0.0013	
16	☑	★	Vimentin OS=Rattus norvegicus OX=10116 GN=Vim PE=1 SV=2	P31000	Vim	54 kDa	★	0.0014	
17	☑	★	Prothymosin alpha OS=Rattus norvegicus OX=10116 GN=Ptma PE=1 SV=2	P06302	Ptma	12 kDa		0.0016	
18	☑	★	Adducin 1 (Alpha), isoform CRA_b OS=Rattus norvegicus OX=10116 GN=Add1 PE=1 SV=1	A0A0G2J5...	Add1	80 kDa		0.0016	
19	☑	★	LIM and SH3 domain protein 1 OS=Rattus norvegicus OX=10116 GN=Lasp1 PE=1 SV=1	Q99MZ8	Lasp1	30 kDa		0.0016	
20	☑	★	Spectrin beta chain OS=Rattus norvegicus OX=10116 GN=Sptbn1 PE=1 SV=1	A0A0G2K8...	Sptbn1	273 kDa	★	0.0019	
21	☑	★	Enhancer of mRNA-decapping protein 4 OS=Rattus norvegicus OX=10116 GN=Edc4 PE=1 SV=2	F7F707 (+1)	Edc4	163 kDa		0.0019	
22	☑	☆	14-3-3 protein gamma OS=Rattus norvegicus OX=10116 GN=Ywhag PE=1 SV=2	P61983	Ywhag	28 kDa	★	0.0020	
23	☑	★	Clathrin heavy chain 1 OS=Rattus norvegicus OX=10116 GN=Cltc PE=1 SV=3	P11442	Cltc	192 kDa		0.0020	
24	☑	★	Heterogeneous nuclear ribonucleoprotein L OS=Rattus norvegicus OX=10116 GN=Hnrnpl PE=1 SV=2	F1LQ48	Hnrnpl	68 kDa		0.0020	
25	☑	★	Malate dehydrogenase, mitochondrial OS=Rattus norvegicus OX=10116 GN=Mdh2 PE=1 SV=2	P04636	Mdh2	36 kDa		0.0021	
26	☑	★	Histone H1.5 OS=Rattus norvegicus OX=10116 GN=H1-5 PE=1 SV=1	D3ZBN0	H1-5	23 kDa	★	0.0022	
27	☑	★	40S ribosomal protein S28 OS=Rattus norvegicus OX=10116 GN=Rps28 PE=1 SV=1	P62859	Rps28	8 kDa		0.0023	
28	☑	★	Septin 7 OS=Rattus norvegicus OX=10116 GN=Sept7 PE=2 SV=1	A2VCW8	Sept7	51 kDa		0.0024	
29	☑	★	ATP synthase subunit O, mitochondrial OS=Rattus norvegicus OX=10116 GN=Atp5po PE=1 SV=1	Q06647	Atp5po	23 kDa		0.0024	
30	☑	★	Far upstream element-binding protein 2 OS=Rattus norvegicus OX=10116 GN=Khsrp PE=1 SV=1	A0A0G2K2...	Khsrp	77 kDa	★	0.0025	
31	☑	★	Calcium-regulated heat stable protein 1 OS=Rattus norvegicus OX=10116 GN=Carhsp1 PE=1 SV=1	Q9WU49	Carhsp1	16 kDa		0.0027	
32	☑	★	14-3-3 protein epsilon OS=Rattus norvegicus OX=10116 GN=Ywhae PE=1 SV=1	P62260	Ywhae	29 kDa	★	0.0028	
33	☑	★	Nuclear autoantigenic sperm protein OS=Rattus norvegicus OX=10116 GN=Nasp PE=1 SV=1	Q66HD3	Nasp	84 kDa		0.0029	
34	☑	★	Myristoylated alanine-rich C-kinase substrate OS=Rattus norvegicus OX=10116 GN=Marcks PE=1 SV=2	P30009	Marcks	30 kDa		0.0029	

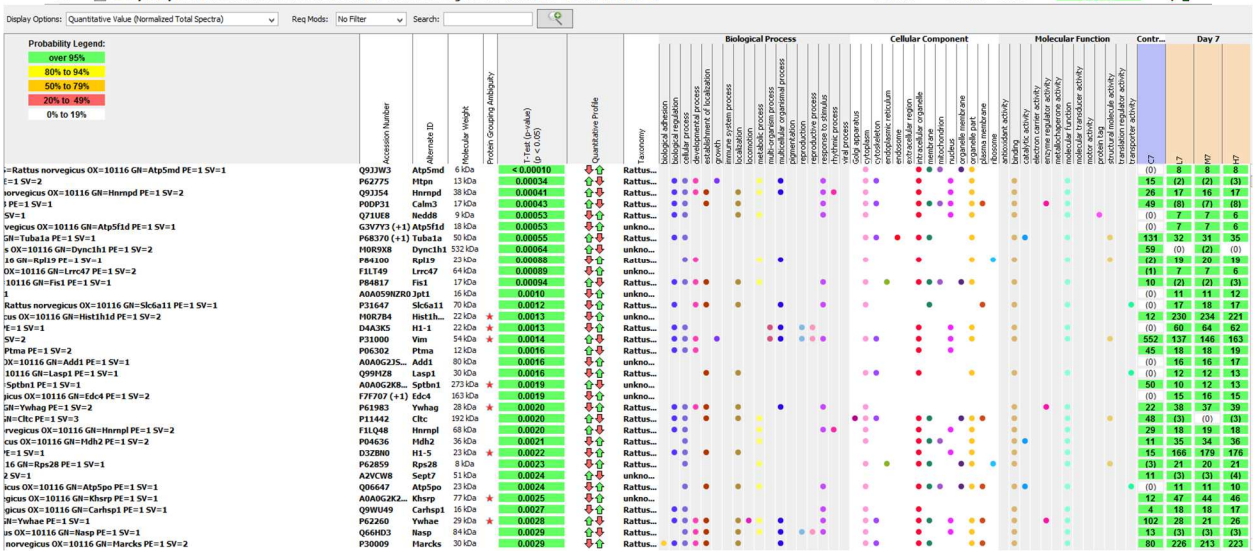

Display Options: Quantitative Value (Normalized Total Spectra) | Req Mods: No Filter | Search:

Probability Legend:
over 95%
80% to 94%
50% to 79%
20% to 49%
0% to 19%

Biological Process | Cellular Component | Molecular Function | Contr... | Day 7

	Accession Number	Alternate ID	Molecular Weight	Protein Grouping Ambiguity	T-Test (p-value) (p < 0.05)	Quantitative Profile	Taxonomy	C7	L7	M7	H7
=Rattus norvegicus OX=10116 GN=Atp5md PE=1 SV=1	Q9JJW3	Atp5md	6 kDa		< 0.00010		Rattus...	(0)	8	8	8
E=1 SV=2	P62775	Mtpn	13 kDa		0.00034		Rattus...	15	(2)	(2)	(3)
norvegicus OX=10116 GN=Hnrnpd PE=1 SV=2	Q9JJ54	Hnrnpd	38 kDa		0.00041		Rattus...	26	17	16	17
) PE=1 SV=1	P0DP31	Calm3	17 kDa		0.00043		Rattus...	49	(8)	(7)	(8)
SV=1	Q71UE8	Nedd8	9 kDa		0.00053		Rattus...	(0)	7	7	6
vegicus OX=10116 GN=Atp5f1d PE=1 SV=1	G3V7Y3 (+1)	Atp5f1d	18 kDa		0.00053		unkno...	(0)	7	7	6
GN=Tuba1a PE=1 SV=1	P68370 (+1)	Tuba1a	50 kDa		0.00055		Rattus...	131	32	31	35
s OX=10116 GN=Dync1h1 PE=1 SV=2	M0R9X8	Dync1h1	532 kDa		0.00064		unkno...	59	(0)	(2)	(0)
16 GN=Rpl19 PE=1 SV=1	P84100	Rpl19	23 kDa		0.00088		Rattus...	(2)	19	20	19
OX=10116 GN=Lrrc47 PE=1 SV=2	F1LT49	Lrrc47	64 kDa		0.00089		unkno...	(1)	7	7	6
10116 GN=Fis1 PE=1 SV=1	P84817	Fis1	17 kDa		0.00094		Rattus...	10	(2)	(2)	(3)
1	A0A059NZR0	Jpt1	16 kDa		0.0010		unkno...	(0)	11	11	12
Rattus norvegicus OX=10116 GN=Slc6a11 PE=1 SV=1	P31647	Slc6a11	70 kDa		0.0012		Rattus...	(0)	17	18	17
us OX=10116 GN=Hist1h1d PE=1 SV=2	M0R7B4	Hist1h...	22 kDa	★	0.0013		unkno...	12	230	234	221
E=1 SV=1	D4A3K5	H1-1	22 kDa	★	0.0013		Rattus...	(0)	60	64	62
SV=2	P31000	Vim	54 kDa	★	0.0014		Rattus...	552	137	146	163
Ptma PE=1 SV=2	P06302	Ptma	12 kDa		0.0016		Rattus...	45	18	18	19
OX=10116 GN=Add1 PE=1 SV=1	A0A0G2J5...	Add1	80 kDa		0.0016		unkno...	(0)	16	16	17
10116 GN=Lasp1 PE=1 SV=1	Q99MZ8	Lasp1	30 kDa		0.0016		Rattus...	(0)	12	12	13
Sptbn1 PE=1 SV=1	A0A0G2K8...	Sptbn1	273 kDa	★	0.0019		unkno...	50	10	12	13
jicus OX=10116 GN=Edc4 PE=1 SV=2	F7F707 (+1)	Edc4	163 kDa		0.0019		unkno...	(0)	15	16	15
GN=Ywhag PE=1 SV=2	P61983	Ywhag	28 kDa	★	0.0020		Rattus...	22	38	37	39
N=Cltc PE=1 SV=3	P11442	Cltc	192 kDa		0.0020		Rattus...	48	(3)	(0)	(3)
rvegicus OX=10116 GN=Hnrnpl PE=1 SV=2	F1LQ48	Hnrnpl	68 kDa		0.0020		Rattus...	29	18	19	18
cus OX=10116 GN=Mdh2 PE=1 SV=2	P04636	Mdh2	36 kDa		0.0021		Rattus...	11	35	34	36
E=1 SV=1	D3ZBN0	H1-5	23 kDa	★	0.0022		Rattus...	15	166	179	176
16 GN=Rps28 PE=1 SV=1	P62859	Rps28	8 kDa		0.0023		Rattus...	(3)	21	20	21
2 SV=1	A2VCW8	Sept7	51 kDa		0.0024		unkno...	11	(3)	(3)	(4)
icus OX=10116 GN=Atp5po PE=1 SV=1	Q06647	Atp5po	23 kDa		0.0024		Rattus...	(0)	11	11	10
gicus OX=10116 GN=Khsrp PE=1 SV=1	A0A0G2K2...	Khsrp	77 kDa	★	0.0025		unkno...	12	47	44	46
gicus OX=10116 GN=Carhsp1 PE=1 SV=1	Q9WU49	Carhsp1	16 kDa		0.0027		Rattus...	4	18	18	17
N=Ywhae PE=1 SV=1	P62260	Ywhae	29 kDa	★	0.0028		Rattus...	102	28	21	26
s OX=10116 GN=Nasp PE=1 SV=1	Q66HD3	Nasp	84 kDa		0.0029		Rattus...	13	(3)	(3)	(3)
norvegicus OX=10116 GN=Marcks PE=1 SV=2	P30009	Marcks	30 kDa		0.0029		Rattus...	80	226	213	223

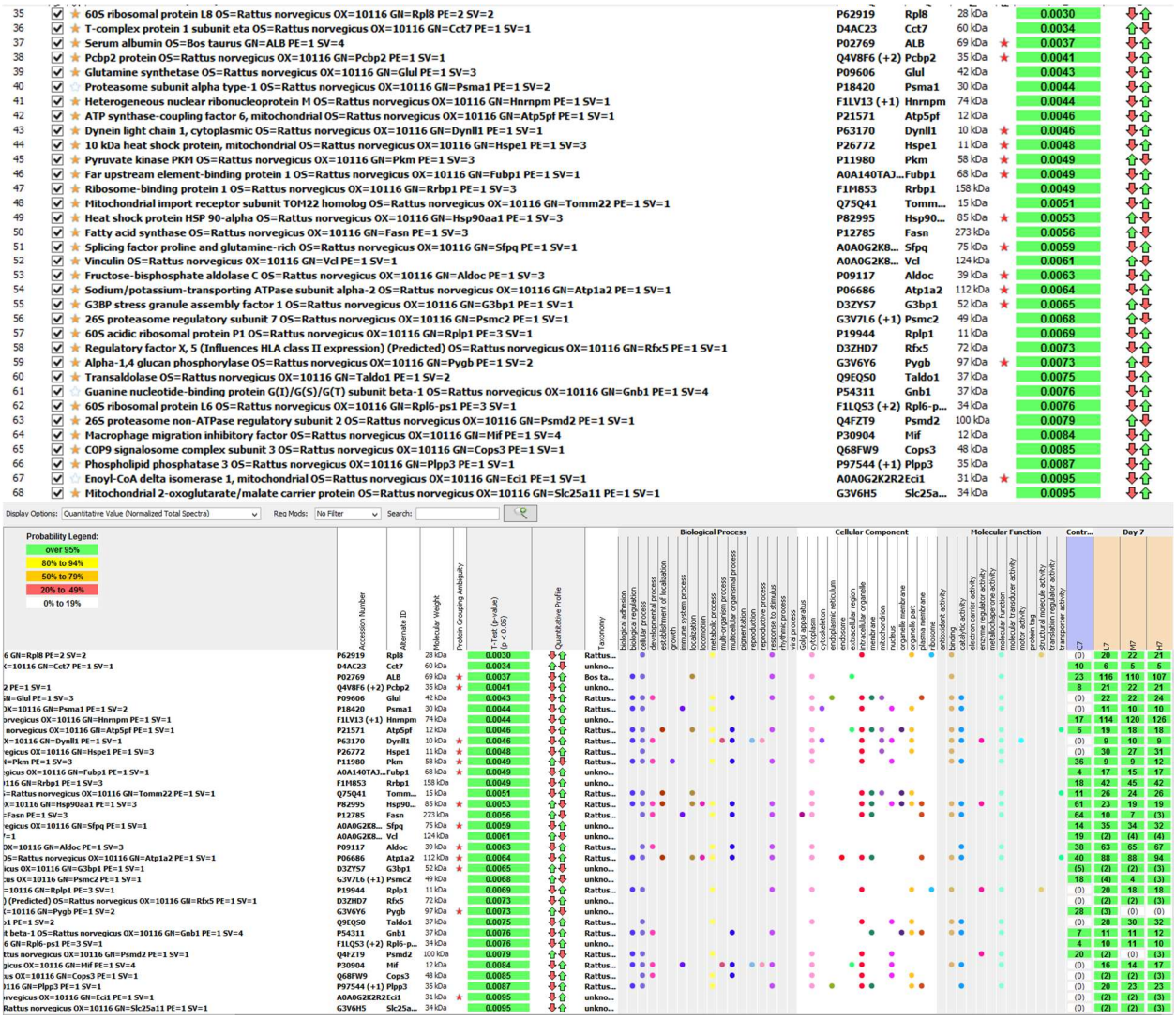

35	60S ribosomal protein L8 OS=Rattus norvegicus OX=10116 GN=Rpl8 PE=2 SV=2	P62919	Rpl8	28 kDa		0.0030		
36	T-complex protein 1 subunit eta OS=Rattus norvegicus OX=10116 GN=Cct7 PE=1 SV=1	D4AC23	Cct7	60 kDa		0.0034		
37	Serum albumin OS=Bos taurus GN=ALB PE=1 SV=4	P02769	ALB	69 kDa	★	0.0037		
38	Pcbp2 protein OS=Rattus norvegicus OX=10116 GN=Pcbp2 PE=1 SV=1	Q4V8F6 (+2)	Pcbp2	35 kDa	★	0.0041		
39	Glutamine synthetase OS=Rattus norvegicus OX=10116 GN=Glul PE=1 SV=3	P09606	Glul	42 kDa		0.0043		
40	Proteasome subunit alpha type-1 OS=Rattus norvegicus OX=10116 GN=Psma1 PE=1 SV=2	P18420	Psma1	30 kDa		0.0044		
41	Heterogeneous nuclear ribonucleoprotein M OS=Rattus norvegicus OX=10116 GN=Hnrnpm PE=1 SV=1	F1LV13 (+1)	Hnrnpm	74 kDa		0.0044		
42	ATP synthase-coupling factor 6, mitochondrial OS=Rattus norvegicus OX=10116 GN=Atp5pf PE=1 SV=1	P21571	Atp5pf	12 kDa		0.0046		
43	Dynein light chain 1, cytoplasmic OS=Rattus norvegicus OX=10116 GN=Dynll1 PE=1 SV=1	P63170	Dynll1	10 kDa	★	0.0046		
44	10 kDa heat shock protein, mitochondrial OS=Rattus norvegicus OX=10116 GN=Hspe1 PE=1 SV=3	P26772	Hspe1	11 kDa	★	0.0048		
45	Pyruvate kinase PKM OS=Rattus norvegicus OX=10116 GN=Pkm PE=1 SV=3	P11980	Pkm	58 kDa	★	0.0049		
46	Far upstream element-binding protein 1 OS=Rattus norvegicus OX=10116 GN=Fubp1 PE=1 SV=1	A0A140TAJ...	Fubp1	68 kDa	★	0.0049		
47	Ribosome-binding protein 1 OS=Rattus norvegicus OX=10116 GN=Rrbp1 PE=1 SV=3	F1M853	Rrbp1	158 kDa		0.0049		
48	Mitochondrial import receptor subunit TOM22 homolog OS=Rattus norvegicus OX=10116 GN=Tomm22 PE=1 SV=1	Q75Q41	Tomm...	15 kDa		0.0051		
49	Heat shock protein HSP 90-alpha OS=Rattus norvegicus OX=10116 GN=Hsp90aa1 PE=1 SV=3	P82995	Hsp90...	85 kDa	★	0.0053		
50	Fatty acid synthase OS=Rattus norvegicus OX=10116 GN=Fasn PE=1 SV=3	P12785	Fasn	273 kDa		0.0056		
51	Splicing factor proline and glutamine-rich OS=Rattus norvegicus OX=10116 GN=Sfpq PE=1 SV=1	A0A0G2K8...	Sfpq	75 kDa	★	0.0059		
52	Vinculin OS=Rattus norvegicus OX=10116 GN=Vcl PE=1 SV=1	A0A0G2K8...	Vcl	124 kDa		0.0061		
53	Fructose-bisphosphate aldolase C OS=Rattus norvegicus OX=10116 GN=Aldoc PE=1 SV=3	P09117	Aldoc	39 kDa	★	0.0063		
54	Sodium/potassium-transporting ATPase subunit alpha-2 OS=Rattus norvegicus OX=10116 GN=Atp1a2 PE=1 SV=1	P06686	Atp1a2	112 kDa	★	0.0064		
55	G3BP stress granule assembly factor 1 OS=Rattus norvegicus OX=10116 GN=G3bp1 PE=1 SV=1	D3ZYS7	G3bp1	52 kDa	★	0.0065		
56	26S proteasome regulatory subunit 7 OS=Rattus norvegicus OX=10116 GN=Psmc2 PE=1 SV=1	G3V7L6 (+1)	Psmc2	49 kDa		0.0068		
57	60S acidic ribosomal protein P1 OS=Rattus norvegicus OX=10116 GN=Rplp1 PE=3 SV=1	P19944	Rplp1	11 kDa		0.0069		
58	Regulatory factor X, 5 (Influences HLA class II expression) (Predicted) OS=Rattus norvegicus OX=10116 GN=Rfx5 PE=1 SV=1	D3ZHD7	Rfx5	72 kDa		0.0073		
59	Alpha-1,4 glucan phosphorylase OS=Rattus norvegicus OX=10116 GN=Pygb PE=1 SV=2	G3V6Y6	Pygb	97 kDa	★	0.0073		
60	Transaldolase OS=Rattus norvegicus OX=10116 GN=Taldo1 PE=1 SV=2	Q9EQS0	Taldo1	37 kDa		0.0075		
61	Guanine nucleotide-binding protein G(I)/G(S)/G(T) subunit beta-1 OS=Rattus norvegicus OX=10116 GN=Gnb1 PE=1 SV=4	P54311	Gnb1	37 kDa		0.0076		
62	60S ribosomal protein L6 OS=Rattus norvegicus OX=10116 GN=Rpl6-ps1 PE=3 SV=1	F1LQS3 (+2)	Rpl6-p...	34 kDa		0.0076		
63	26S proteasome non-ATPase regulatory subunit 2 OS=Rattus norvegicus OX=10116 GN=Psmd2 PE=1 SV=1	Q4FZT9	Psmd2	100 kDa		0.0079		
64	Macrophage migration inhibitory factor OS=Rattus norvegicus OX=10116 GN=Mif PE=1 SV=4	P30904	Mif	12 kDa		0.0084		
65	COP9 signalosome complex subunit 3 OS=Rattus norvegicus OX=10116 GN=Cops3 PE=1 SV=1	Q68FW9	Cops3	48 kDa		0.0085		
66	Phospholipid phosphatase 3 OS=Rattus norvegicus OX=10116 GN=Plpp3 PE=1 SV=1	P97544 (+1)	Plpp3	35 kDa		0.0087		
67	Enoyl-CoA delta isomerase 1, mitochondrial OS=Rattus norvegicus OX=10116 GN=Eci1 PE=1 SV=1	A0A0G2K2R2	Eci1	31 kDa	★	0.0095		
68	Mitochondrial 2-oxoglutarate/malate carrier protein OS=Rattus norvegicus OX=10116 GN=Slc25a11 PE=1 SV=1	G3V6H5	Slc25a...	34 kDa		0.0095		

Display Options: Quantitative Value (Normalized Total Spectra) | Req Mods: No Filter | Search:

Probability Legend: over 95% | 80% to 94% | 50% to 79% | 20% to 49% | 0% to 19%

Biological Process | Cellular Component | Molecular Function | Contr... | Day 7

	Accession Number	Alternate ID	Molecular Weight	Protein Grouping Ambiguity	T-test (p-value) (p < 0.05)	Quantitative Profile	Taxonomy	C7	L7	H7	H7
6 GN=Rpl8 PE=2 SV=2	P62919	Rpl8	28 kDa		0.0030		Rattus...	(0)	20	22	21
K=10116 GN=Cct7 PE=1 SV=1	D4AC23	Cct7	60 kDa		0.0034		unkno...	10	6	5	5
	P02769	ALB	69 kDa	★	0.0037		Bos ta...	23	116	110	107
2 PE=1 SV=1	Q4V8F6 (+2)	Pcbp2	35 kDa	★	0.0041		unkno...	8	21	22	21
N=Glul PE=1 SV=3	P09606	Glul	42 kDa		0.0043		Rattus...	(0)	22	22	24
DX=10116 GN=Psma1 PE=1 SV=2	P18420	Psma1	30 kDa		0.0044		Rattus...	(0)	11	10	10
orvegicus OX=10116 GN=Hnrnpm PE=1 SV=1	F1LV13 (+1)	Hnrnpm	74 kDa		0.0044		unkno...	17	114	120	126
norvegicus OX=10116 GN=Atp5pf PE=1 SV=1	P21571	Atp5pf	12 kDa		0.0046		Rattus...	6	19	18	18
X=10116 GN=Dynll1 PE=1 SV=1	P63170	Dynll1	10 kDa	★	0.0046		Rattus...	(0)	9	10	9
egicus OX=10116 GN=Hspe1 PE=1 SV=3	P26772	Hspe1	11 kDa	★	0.0048		Rattus...	(0)	30	27	31
=Pkm PE=1 SV=3	P11980	Pkm	58 kDa	★	0.0049		Rattus...	36	9	9	12
gicus OX=10116 GN=Fubp1 PE=1 SV=1	A0A140TAJ...	Fubp1	68 kDa	★	0.0049		unkno...	4	17	15	17
116 GN=Rrbp1 PE=1 SV=3	F1M853	Rrbp1	158 kDa		0.0049		unkno...	18	42	45	42
=Rattus norvegicus OX=10116 GN=Tomm22 PE=1 SV=1	Q75Q41	Tomm...	15 kDa		0.0051		Rattus...	11	26	24	26
X=10116 GN=Hsp90aa1 PE=1 SV=3	P82995	Hsp90...	85 kDa	★	0.0053		Rattus...	61	23	19	19
=Fasn PE=1 SV=3	P12785	Fasn	273 kDa		0.0056		Rattus...	64	10	7	(3)
egicus OX=10116 GN=Sfpq PE=1 SV=1	A0A0G2K8...	Sfpq	75 kDa	★	0.0059		unkno...	14	35	34	32
=1	A0A0G2K8...	Vcl	124 kDa		0.0061		unkno...	19	(2)	(4)	(4)
DX=10116 GN=Aldoc PE=1 SV=3	P09117	Aldoc	39 kDa	★	0.0063		Rattus...	38	63	65	67
OS=Rattus norvegicus OX=10116 GN=Atp1a2 PE=1 SV=1	P06686	Atp1a2	112 kDa	★	0.0064		Rattus...	40	88	88	94
icus OX=10116 GN=G3bp1 PE=1 SV=1	D3ZYS7	G3bp1	52 kDa	★	0.0065		unkno...	(5)	(2)	(2)	(3)
cus OX=10116 GN=Psmc2 PE=1 SV=1	G3V7L6 (+1)	Psmc2	49 kDa		0.0068		unkno...	18	(4)	4	(3)
=10116 GN=Rplp1 PE=3 SV=1	P19944	Rplp1	11 kDa		0.0069		Rattus...	(0)	20	18	18
) (Predicted) OS=Rattus norvegicus OX=10116 GN=Rfx5 PE=1 SV=1	D3ZHD7	Rfx5	72 kDa		0.0073		unkno...	(0)	(2)	(2)	(3)
X=10116 GN=Pygb PE=1 SV=2	G3V6Y6	Pygb	97 kDa	★	0.0073		unkno...	28	(3)	(0)	(0)
1 PE=1 SV=2	Q9EQS0	Taldo1	37 kDa		0.0075		Rattus...	(0)	28	30	32
t beta-1 OS=Rattus norvegicus OX=10116 GN=Gnb1 PE=1 SV=4	P54311	Gnb1	37 kDa		0.0076		Rattus...	7	11	11	12
6 GN=Rpl6-ps1 PE=3 SV=1	F1LQS3 (+2)	Rpl6-p...	34 kDa		0.0076		unkno...	4	10	11	10
ttus norvegicus OX=10116 GN=Psmd2 PE=1 SV=1	Q4FZT9	Psmd2	100 kDa		0.0079		Rattus...	20	(2)	(0)	(3)
gicus OX=10116 GN=Mif PE=1 SV=4	P30904	Mif	12 kDa		0.0084		Rattus...	(0)	16	14	17
us OX=10116 GN=Cops3 PE=1 SV=1	Q68FW9	Cops3	48 kDa		0.0085		Rattus...	(0)	(2)	(2)	(3)
116 GN=Plpp3 PE=1 SV=1	P97544 (+1)	Plpp3	35 kDa		0.0087		Rattus...	(0)	20	23	23
rvegicus OX=10116 GN=Eci1 PE=1 SV=1	A0A0G2K2R2	Eci1	31 kDa	★	0.0095		unkno...	(0)	(2)	(2)	(3)
Rattus norvegicus OX=10116 GN=Slc25a11 PE=1 SV=1	G3V6H5	Slc25a...	34 kDa		0.0095		unkno...	(0)	(2)	(2)	(3)

69	Metallothionein OS=Rattus norvegicus OX=10116 GN=Mt1m PE=3 SV=1	D3ZHV3 (+1)	Mt1m	6 kDa		0.0095
70	Acetyl-CoA acetyltransferase, cytosolic OS=Rattus norvegicus OX=10116 GN=Acat2 PE=1 SV=1	Q5XI22	Acat2	41 kDa		0.0096
71	Heterogeneous nuclear ribonucleoprotein A1 OS=Rattus norvegicus OX=10116 GN=Hnrnpa1 PE=1 SV=3	P04256 (+1)	Hnrnpa1	34 kDa	★	0.0099
72	Microtubule-associated protein OS=Rattus norvegicus OX=10116 GN=Map2 PE=1 SV=3	F1LNK0 (+1)	Map2	211 kDa		0.010
73	RCG39700, isoform CRA_d OS=Rattus norvegicus OX=10116 GN=Rab6a PE=1 SV=1	A0A0H2UH...	Rab6a	24 kDa		0.010
74	Peptidylprolyl isomerase OS=Rattus norvegicus OX=10116 GN=Fkbp3 PE=1 SV=1	G3V6L9	Fkbp3	25 kDa		0.011
75	Thioredoxin domain-containing protein OS=Rattus norvegicus OX=10116 PE=4 SV=1	A0A0G2K3...		22 kDa		0.011
76	Acyl-CoA-binding protein OS=Rattus norvegicus OX=10116 GN=Dbi PE=1 SV=3	P11030	Dbi	10 kDa	★	0.011
77	Bifunctional purine biosynthesis protein PURH OS=Rattus norvegicus OX=10116 GN=Atic PE=1 SV=2	O35567	Atic	64 kDa		0.011
78	T-complex protein 1 subunit delta OS=Rattus norvegicus OX=10116 GN=Cct4 PE=1 SV=3	Q7TPB1	Cct4	58 kDa		0.011
79	Parathymosin OS=Rattus norvegicus OX=10116 GN=Ptms PE=1 SV=1	B3DM95	Ptms	12 kDa		0.011
80	Actin, alpha skeletal muscle OS=Rattus norvegicus OX=10116 GN=Acta1 PE=1 SV=1	P68136	Acta1	42 kDa	★	0.011
81	Rho GDP-dissociation inhibitor 1 OS=Rattus norvegicus OX=10116 GN=Arhgdia PE=1 SV=1	Q5XI73	Arhgdia	23 kDa		0.011
82	3-ketoacyl-CoA thiolase, mitochondrial OS=Rattus norvegicus OX=10116 GN=Acaa2 PE=1 SV=1	P13437	Acaa2	42 kDa		0.011
83	Cytochrome c oxidase subunit 4 isoform 1, mitochondrial OS=Rattus norvegicus OX=10116 GN=Cox4i1 PE=1 SV=1	P10888	Cox4i1	20 kDa		0.011
84	NIF3-like protein 1 OS=Rattus norvegicus OX=10116 GN=Nif3l1 PE=1 SV=1	Q4V7D6 (+1)	Nif3l1	42 kDa		0.012
85	Histone H2B OS=Rattus norvegicus OX=10116 GN=LOC102549061 PE=3 SV=1	A0A0G2JXE0	LOC10...	14 kDa	★	0.012
86	Protein phosphatase 2 (Formerly 2A), regulatory subunit A (PR 65), alpha isoform, isoform CRA_a OS=Rattus norvegicus OX=10116 GN=Ppp2r1a...	Q5XI34	Ppp2r1a	65 kDa	★	0.012
87	Cortactin, isoform CRA_c OS=Rattus norvegicus OX=10116 GN=Cttn PE=1 SV=3	D3ZGE6 (+1)	Cttn	61 kDa		0.012
88	Nucleolin OS=Rattus norvegicus OX=10116 GN=Ncl PE=1 SV=3	P13383 (+1)	Ncl	77 kDa		0.013
89	60S ribosomal protein L28 OS=Rattus norvegicus OX=10116 GN=Rpl28 PE=2 SV=1	Q642E2	Rpl28	16 kDa		0.013
90	Reticulon OS=Rattus norvegicus OX=10116 GN=Rtn3 PE=1 SV=1	A0A0H2UH...	Rtn3	28 kDa		0.014
91	Ras-related protein Rab-1A OS=Rattus norvegicus OX=10116 GN=Rab1A PE=1 SV=3	Q6NYB7	Rab1A	23 kDa	★	0.014
92	Spectrin alpha chain, non-erythrocytic 1 OS=Rattus norvegicus OX=10116 GN=Sptan1 PE=1 SV=1	A0A0G2JZ69	Sptan1	287 kDa		0.014
93	Glial fibrillary acidic protein OS=Rattus norvegicus OX=10116 GN=Gfap PE=1 SV=2	P47819	Gfap	50 kDa	★	0.014
94	L-lactate dehydrogenase B chain OS=Rattus norvegicus OX=10116 GN=Ldhb PE=1 SV=2	P42123	Ldhb	37 kDa		0.014
95	Core histone macro-H2A OS=Rattus norvegicus OX=10116 GN=H2afy PE=1 SV=1	A0A140TA...	H2afy	39 kDa	★	0.014
96	ADP/ATP translocase 2 OS=Rattus norvegicus OX=10116 GN=Slc25a5 PE=1 SV=3	Q09073	Slc25a5	33 kDa	★	0.014
97	Proteasome subunit alpha type-5 OS=Rattus norvegicus OX=10116 GN=Psma5 PE=1 SV=1	P34064 (+1)	Psma5	26 kDa		0.015
98	Ubiquitin-like modifier-activating enzyme 1 OS=Rattus norvegicus OX=10116 GN=Uba1 PE=1 SV=1	Q5U300	Uba1	118 kDa		0.015
99	L-lactate dehydrogenase A chain OS=Rattus norvegicus OX=10116 GN=Ldha PE=1 SV=1	P04642	Ldha	36 kDa		0.015
100	ATP synthase subunit beta, mitochondrial OS=Rattus norvegicus OX=10116 GN=Atp5f1b PE=1 SV=2	P10719	Atp5f1b	56 kDa		0.015
101	Uncharacterized protein OS=Rattus norvegicus OX=10116 PE=4 SV=2	D3Z525 (+1)		24 kDa	★	0.015
102	RNA-binding motif protein, X chromosome retrogene-like OS=Rattus norvegicus OX=10116 GN=Rbmxrtl PE=1 SV=1	P84586	Rbmxrtl	42 kDa	★	0.016

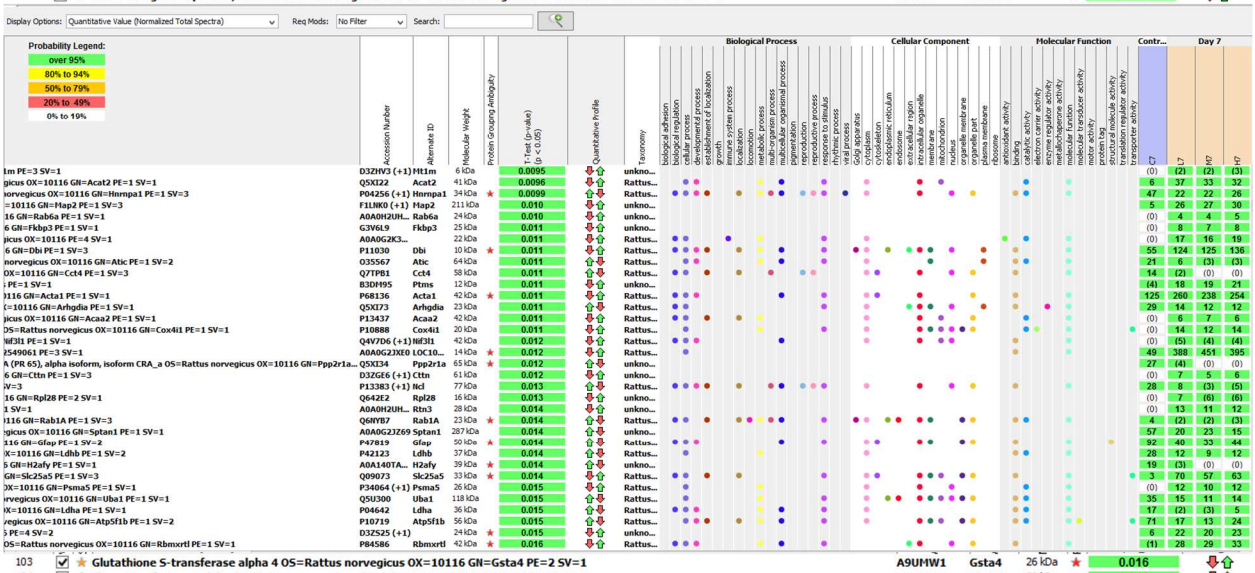

103	Glutathione S-transferase alpha 4 OS=Rattus norvegicus OX=10116 GN=Gsta4 PE=2 SV=1	A9UMW1	Gsta4	26 kDa	★	0.016
104	Elongation factor 1-alpha OS=Rattus norvegicus OX=10116 GN=LOC100360413 PE=3 SV=1	M0R757	LOC10...	50 kDa		0.016
105	60S ribosomal protein L24 OS=Rattus norvegicus OX=10116 GN=Rpl24 PE=1 SV=1	A0A0H2UH...	Rpl24	18 kDa		0.016
106	Histone H1.4 OS=Rattus norvegicus OX=10116 GN=H1-4 PE=1 SV=3	P15865	H1-4	22 kDa	★	0.016
107	Histidine triad nucleotide-binding protein 1 OS=Rattus norvegicus OX=10116 GN=Hint1 PE=1 SV=5	P62959	Hint1	14 kDa		0.016
108	Heterogeneous nuclear ribonucleoproteins A2/B1 OS=Rattus norvegicus OX=10116 GN=Hnrnpa2b1 PE=1 SV=1	F1LNF1	Hnrnp...	37 kDa	★	0.017
109	Protein phosphatase 1 regulatory subunit 14B OS=Rattus norvegicus OX=10116 GN=Ppp1r14b PE=2 SV=1	Q8K3F3	Ppp1r1...	16 kDa		0.017
110	Isoaspartyl peptidase/L-asparaginase OS=Rattus norvegicus OX=10116 GN=Asrgl1 PE=1 SV=1	Q8VI04	Asrgl1	34 kDa		0.017
111	Sodium/potassium-transporting ATPase subunit beta OS=Rattus norvegicus OX=10116 GN=Atp1b2 PE=1 SV=1	Q5M9H4	Atp1b2	33 kDa		0.017
112	Far upstream element-binding protein 3 OS=Rattus norvegicus OX=10116 GN=Fubp3 PE=1 SV=1	G3V829	Fubp3	61 kDa	★	0.018
113	40S ribosomal protein S12 OS=Rattus norvegicus OX=10116 GN=Rps12 PE=1 SV=2	P63324	Rps12	15 kDa	★	0.018
114	Microtubule-associated protein OS=Rattus norvegicus OX=10116 GN=Map4 PE=1 SV=1	A0A0G2JW...	Map4	233 kDa	★	0.018
115	Heterogeneous nuclear ribonucleoprotein U OS=Rattus norvegicus OX=10116 GN=Hnrnpu PE=1 SV=1	A0A0G2JZ5...	Hnrnpu	88 kDa		0.018
116	ATP synthase subunit f, mitochondrial OS=Rattus norvegicus OX=10116 GN=Atp5mf PE=1 SV=1	D3ZAF6	Atp5mf	10 kDa		0.018
117	RCG61099, isoform CRA_b OS=Rattus norvegicus OX=10116 GN=Srsf3 PE=1 SV=1	A0A0U1RR...	Srsf3	14 kDa	★	0.019
118	Rat glutathione S-transferase OS=Rattus norvegicus OX=10116 PE=2 SV=1	Q6LDP3		26 kDa	★	0.021
119	Acidic leucine-rich nuclear phosphoprotein 32 family member A OS=Rattus norvegicus OX=10116 GN=Anp32a PE=1 SV=1	A0A0G2K7...	Anp32a	26 kDa		0.022
120	Reticulon OS=Rattus norvegicus OX=10116 GN=Rtn4 PE=1 SV=1	F1LQN3 (+1)	Rtn4	126 kDa		0.023
121	RCG45615, isoform CRA_a OS=Rattus norvegicus OX=10116 GN=Rpl12 PE=2 SV=1	B2RYU2	Rpl12	18 kDa		0.023
122	ATP synthase protein 8 OS=Rattus norvegicus OX=10116 GN=ATP8 PE=3 SV=1	Q5UAJ5	ATP8	8 kDa		0.023
123	Histone H2A type 1-C OS=Rattus norvegicus OX=10116 PE=1 SV=2	P0C169		14 kDa	★	0.023
124	Cell division control protein 42 homolog OS=Rattus norvegicus OX=10116 GN=Cdc42 PE=1 SV=2	Q8CFN2	Cdc42	21 kDa		0.024
125	Myelin expression factor 2 OS=Rattus norvegicus OX=10116 GN=Myef2 PE=1 SV=1	A0A0G2K4...	Myef2	63 kDa		0.024
126	Splicing factor 3b, subunit 1 OS=Rattus norvegicus OX=10116 GN=Sf3b1 PE=1 SV=1	G3V7T6	Sf3b1	146 kDa		0.024
127	Sodium/potassium-transporting ATPase subunit alpha-1 OS=Rattus norvegicus OX=10116 GN=Atp1a1 PE=1 SV=1	P06685	Atp1a1	113 kDa	★	0.024
128	Neural cell adhesion molecule 1 OS=Rattus norvegicus OX=10116 GN=Ncam1 PE=1 SV=1	P13596	Ncam1	95 kDa		0.025
129	Elongation factor 2 OS=Rattus norvegicus OX=10116 GN=Eef2 PE=1 SV=4	P05197	Eef2	95 kDa	★	0.025
130	Heterogeneous nuclear ribonucleoprotein A3 OS=Rattus norvegicus OX=10116 GN=Hnrnpa3 PE=1 SV=1	Q6URK4	Hnrnpa3	40 kDa	★	0.026
131	Phosphate carrier protein, mitochondrial OS=Rattus norvegicus OX=10116 GN=Slc25a3 PE=1 SV=1	G3V741 (+1)	Slc25a3	40 kDa		0.026
132	Fatty acid-binding protein 5 OS=Rattus norvegicus OX=10116 GN=Fabp5 PE=1 SV=3	P55053	Fabp5	15 kDa		0.026
133	Heat shock cognate 71 kDa protein OS=Rattus norvegicus OX=10116 GN=Hspa8 PE=3 SV=3	D4A4S3 (+1)	Hspa8	71 kDa	★	0.027
134	Chromodomain helicase DNA-binding protein 4 OS=Rattus norvegicus OX=10116 GN=Chd4 PE=1 SV=3	E9PU01	Chd4	218 kDa	★	0.027
135	60S ribosomal protein L4 OS=Rattus norvegicus OX=10116 GN=Rpl4 PE=1 SV=1	Q6P3V9	Rpl4	47 kDa		0.027
136	Histone cluster 1 H1 family member c OS=Rattus norvegicus OX=10116 GN=Hist1h1c PE=1 SV=1	A0A0G2K654	Hist1h1c	21 kDa	★	0.028

#			Protein	Accession Number	Alternate ID	Molecular Weight	Protein Grouping Ambiguity	T-Test (p-value) (p < 0.05)	Quantitative Profile
137	☑	★	GMP synthase [glutamine-hydrolyzing] OS=Rattus norvegicus OX=10116 GN=Gmps PE=1 SV=1	Q4V7C6	Gmps	77 kDa		0.028	⇧⇩
138	☑	★	Astrocytic phosphoprotein PEA-15 OS=Rattus norvegicus OX=10116 GN=Pea15 PE=1 SV=1	Q5U318	Pea15	15 kDa		0.029	⇧⇩
139	☑	★	Lamin-B1 OS=Rattus norvegicus OX=10116 GN=Lmnb1 PE=1 SV=1	G3V7U4	Lmnb1	67 kDa	★	0.029	⇧⇩
140	☑	★	Large neutral amino acids transporter small subunit 1 OS=Rattus norvegicus OX=10116 GN=Slc7a5 PE=1 SV=2	Q63016	Slc7a5	56 kDa		0.030	⇩⇧
141	☑	★	Transitional endoplasmic reticulum ATPase OS=Rattus norvegicus OX=10116 GN=Vcp PE=1 SV=3	P46462	Vcp	89 kDa		0.030	⇧⇩
142	☑	★	60S ribosomal protein L13 OS=Rattus norvegicus OX=10116 GN=Rpl13 PE=1 SV=2	P41123	Rpl13	24 kDa		0.030	⇩⇧
143	☑	★	14-3-3 protein beta/alpha OS=Rattus norvegicus OX=10116 GN=Ywhab PE=1 SV=3	P35213	Ywhab	28 kDa	★	0.030	⇩⇧
144	☑	★	Dolichyl-diphosphooligosaccharide--protein glycosyltransferase subunit 1 OS=Rattus norvegicus OX=10116 GN=Rpn1 PE=2 SV=1	P07153 (+1)	Rpn1	68 kDa		0.030	⇩⇧
145	☑	★	Na(+)/H(+) exchange regulatory cofactor NHE-RF1 OS=Rattus norvegicus OX=10116 GN=Slc9a3r1 PE=1 SV=3	Q9JJ19	Slc9a3r1	39 kDa		0.030	⇩⇧
146	☑	☆	Activated RNA polymerase II transcriptional coactivator p15 OS=Rattus norvegicus OX=10116 GN=Sub1 PE=1 SV=3	Q63396	Sub1	14 kDa		0.031	⇩⇧
147	☑	★	Protein-L-isoaspartate O-methyltransferase OS=Rattus norvegicus OX=10116 GN=Pcmt1 PE=1 SV=1	A0A140TA...	Pcmt1	21 kDa		0.031	⇩⇧
148	☑	★	MICOS complex subunit MIC60 OS=Rattus norvegicus OX=10116 GN=Immt PE=1 SV=1	A0A0G2JVH4	Immt	86 kDa		0.031	⇧⇩
149	☑	★	Non-histone chromosomal protein HMG-17 OS=Rattus norvegicus OX=10116 GN=Hmgn2 PE=1 SV=2	P18437	Hmgn2	9 kDa	★	0.031	⇩⇧
150	☑	★	Protein disulfide-isomerase OS=Rattus norvegicus OX=10116 GN=Pdia3 PE=1 SV=1	A0A0H2UH...	Pdia3	57 kDa		0.031	⇩⇧
151	☑	☆	Phytanoyl-CoA hydroxylase-interacting protein-like OS=Rattus norvegicus OX=10116 GN=Phyhipl PE=1 SV=2	Q6AYN4	Phyhipl	42 kDa		0.031	⇩⇧
152	☑	★	S-phase kinase-associated protein 1 OS=Rattus norvegicus OX=10116 GN=Skp1 PE=1 SV=1	A0A0G2K4...	Skp1	19 kDa		0.031	⇧⇩
153	☑	★	Filamin A OS=Rattus norvegicus OX=10116 GN=Flna PE=1 SV=1	C0JPT7	Flna	280 kDa	★	0.032	⇩⇧
154	☑	★	Splicing factor 3b, subunit 2 OS=Rattus norvegicus OX=10116 GN=Sf3b2 PE=1 SV=3	D3ZMS1	Sf3b2	98 kDa		0.032	⇩⇧
155	☑	★	Tropomodulin-2 OS=Rattus norvegicus OX=10116 GN=Tmod2 PE=1 SV=1	P70566	Tmod2	39 kDa		0.032	⇧⇩
156	☑	★	Calponin-3 OS=Rattus norvegicus OX=10116 GN=Cnn3 PE=1 SV=1	P37397	Cnn3	36 kDa	★	0.032	⇩⇧
157	☑	☆	60S ribosomal protein L14 OS=Rattus norvegicus OX=10116 GN=Rpl14 PE=1 SV=1	B5DEM5 (+2)	Rpl14	24 kDa		0.033	⇩⇧
158	☑	★	60S ribosomal protein L34 OS=Rattus norvegicus OX=10116 GN=Rpl34 PE=1 SV=1	B2RZD4	Rpl34	13 kDa		0.033	⇩⇧
159	☑	☆	Phosphoglycerate kinase 1 OS=Rattus norvegicus OX=10116 GN=Pgk1 PE=1 SV=2	P16617	Pgk1	45 kDa	★	0.033	⇩⇧
160	☑	★	Tubulin beta-5 chain OS=Rattus norvegicus OX=10116 GN=Tubb5 PE=1 SV=1	P69897	Tubb5	50 kDa	★	0.034	⇧⇩
161	☑	☆	40S ribosomal protein S25 OS=Rattus norvegicus OX=10116 GN=Rps25 PE=2 SV=1	P62853	Rps25	14 kDa		0.035	⇩⇧
162	☑	☆	Peroxiredoxin-2 OS=Rattus norvegicus OX=10116 GN=Prdx2 PE=1 SV=1	A0A0G2JSH9	Prdx2	22 kDa		0.035	⇩⇧
163	☑	★	Dynactin subunit 2 OS=Rattus norvegicus OX=10116 GN=Dctn2 PE=1 SV=1	A0A0G2JU...	Dctn2	46 kDa		0.035	⇩⇧
164	☑	★	Protein/nucleic acid deglycase DJ-1 OS=Rattus norvegicus OX=10116 GN=Park7 PE=1 SV=1	O88767	Park7	20 kDa		0.035	⇩⇧
165	☑	★	Vesicle-associated membrane protein-associated protein A OS=Rattus norvegicus OX=10116 GN=Vapa PE=1 SV=3	Q9Z270	Vapa	28 kDa		0.035	⇧⇩
166	☑	★	Nesprin 1 short isoform OS=Rattus norvegicus OX=10116 GN=Syne1 PE=2 SV=1	A0A5P8DHK4	Syne1	998 kDa		0.036	⇩⇧
167	☑	★	ATP synthase subunit e, mitochondrial OS=Rattus norvegicus OX=10116 GN=Atp5me PE=1 SV=3	P29419	Atp5me	8 kDa		0.036	⇩⇧
168	☑	☆	Thymosin beta OS=Rattus norvegicus OX=10116 GN=Tmsb15b2 PE=2 SV=1	P97563	Tmsb1...	5 kDa		0.036	⇩⇧
169	☑	★	Gap junction alpha-1 protein OS=Rattus norvegicus OX=10116 GN=Gja1 PE=1 SV=2	P08050	Gja1	43 kDa		0.037	⇩⇧
170	☑	☆	RCG34610, isoform CRA_c OS=Rattus norvegicus OX=10116 GN=Srsf1 PE=1 SV=1	D4A9L2	Srsf1	28 kDa		0.037	⇩⇧

171	Serine/threonine-protein kinase PAK 2 OS=Rattus norvegicus OX=10116 GN=Pak2 PE=1 SV=1	Q64303	Pak2	58 kDa		0.038		
172	Protein quaking OS=Rattus norvegicus OX=10116 GN=Qki PE=1 SV=2	Q91XU1	Qki	38 kDa		0.038		
173	Endoplasmin OS=Rattus norvegicus OX=10116 GN=Hsp90b1 PE=1 SV=1	A0A0A0MY...	Hsp90b1	93 kDa	★	0.038		
174	60S acidic ribosomal protein P2 OS=Rattus norvegicus OX=10116 GN=Rplp2 PE=1 SV=2	P02401	Rplp2	12 kDa		0.038		
175	Heat shock protein HSP 90-beta OS=Rattus norvegicus OX=10116 GN=Hsp90ab1 PE=1 SV=4	P34058	Hsp90...	83 kDa	★	0.038		
176	Ras-related C3 botulinum toxin substrate 1 OS=Rattus norvegicus OX=10116 GN=Rac1 PE=1 SV=1	A0A0G2K0...	Rac1	24 kDa		0.039		
177	Fatty acid-binding protein, brain OS=Rattus norvegicus OX=10116 GN=Fabp7 PE=1 SV=2	P55051	Fabp7	15 kDa		0.039		
178	Aly/REF export factor OS=Rattus norvegicus OX=10116 GN=Alyref PE=1 SV=1	D3ZXH7	Alyref	20 kDa		0.040		
179	Hepatocyte cell adhesion molecule OS=Rattus norvegicus OX=10116 GN=Hepacam PE=1 SV=2	D3ZEI4	Hepac...	47 kDa		0.040		
180	Cullin-associated NEDD8-dissociated protein 1 OS=Rattus norvegicus OX=10116 GN=Cand1 PE=1 SV=1	P97536	Cand1	136 kDa		0.040		
181	Actin, cytoplasmic 1 OS=Rattus norvegicus OX=10116 GN=Actb PE=1 SV=1	P60711 (+1)	Actb	42 kDa	★	0.040		
182	Uncharacterized protein OS=Rattus norvegicus OX=10116 PE=4 SV=1	D4A412		15 kDa	★	0.041		
183	40S ribosomal protein S20 OS=Rattus norvegicus OX=10116 GN=Rps20 PE=3 SV=1	A0A0H2UH...	Rps20	13 kDa		0.041		
184	D-3-phosphoglycerate dehydrogenase OS=Rattus norvegicus OX=10116 GN=Phgdh PE=1 SV=3	O08651	Phgdh	56 kDa		0.041		
185	Fructose-bisphosphate aldolase A OS=Rattus norvegicus OX=10116 GN=Aldoa PE=1 SV=2	P05065	Aldoa	39 kDa	★	0.042		
186	Matrin-3 OS=Rattus norvegicus OX=10116 GN=Matr3 PE=1 SV=2	P43244	Matr3	94 kDa		0.042		
187	Microtubule-associated protein RP/EB family member 1 OS=Rattus norvegicus OX=10116 GN=Mapre1 PE=1 SV=3	Q66HR2	Mapre1	30 kDa	★	0.043		
188	Rab GDP dissociation inhibitor alpha OS=Rattus norvegicus OX=10116 GN=Gdi1 PE=1 SV=1	P50398	Gdi1	51 kDa	★	0.043		
189	40S ribosomal protein S14 OS=Rattus norvegicus OX=10116 GN=Rps14 PE=2 SV=3	P13471 (+1)	Rps14	16 kDa		0.046		
190	Protein disulfide-isomerase A6 OS=Rattus norvegicus OX=10116 GN=Pdia6 PE=1 SV=1	A0A0G2JSZ...	Pdia6	49 kDa		0.047		
191	Catalase OS=Rattus norvegicus OX=10116 GN=Cat PE=1 SV=3	P04762	Cat	60 kDa	★	0.047		
192	FUS RNA-binding protein OS=Rattus norvegicus OX=10116 GN=Fus PE=1 SV=1	Q5PQK2	Fus	53 kDa	★	0.050		
193	4F2 cell-surface antigen heavy chain OS=Rattus norvegicus OX=10116 GN=Slc3a2 PE=1 SV=1	Q794F9	Slc3a2	58 kDa		0.050		

APPENDIX C: LIST OF ANOVA SIGNIFICANT PROTEINS AND FOLD CHANGES IN DAY 3 AND 7 GROUPS

69	Lamina-associated polypeptide 2, isoform beta OS=Rattus norvegicus OX=10116 GN=Tmpo PE=1 SV=3	Q62733	Tmpo	50 kDa		0.00...
70	Sodium/potassium-transporting ATPase subunit alpha-2 OS=Rattus norvegicus OX=10116 GN=Atp1a2 PE=1 SV=1	P06686	Atp1a2	112 kDa	★	0.00...
71	ADP/ATP translocase 1 OS=Rattus norvegicus OX=10116 GN=Slc25a4 PE=1 SV=1	Q6P9Y4	Slc25a4	33 kDa	★	0.00...
72	Reticulon OS=Rattus norvegicus OX=10116 GN=Rtn3 PE=1 SV=1	A0A0H2UH...	Rtn3	28 kDa		0.00...
73	UTP20 small subunit processome component OS=Rattus norvegicus OX=10116 GN=Utp20 PE=1 SV=3	F1LXT3	Utp20	317 kDa		0.012
74	Microtubule-associated protein 4 OS=Rattus norvegicus OX=10116 GN=Map4 PE=1 SV=1	Q5M7W5	Map4	110 kDa	★	0.012
75	Breast carcinoma-amplified sequence 1 homolog OS=Rattus norvegicus OX=10116 GN=Bcas1 PE=1 SV=1	A0A0G2K079	Bcas1	38 kDa	★	0.013
76	Thymosin beta-10 OS=Rattus norvegicus OX=10116 GN=Tmsb10 PE=1 SV=2	P63312	Tmsb10	5 kDa	★	0.013
77	Erythrocyte membrane protein band 4.1-like 2 OS=Rattus norvegicus OX=10116 GN=Epb41l2 PE=1 SV=3	D3ZDT1	Epb41l2	103 kDa	★	0.013
78	60S ribosomal protein L24 OS=Rattus norvegicus OX=10116 GN=Rpl24 PE=2 SV=1	P83732	Rpl24	18 kDa		0.013
79	Splicing factor 1 OS=Rattus norvegicus OX=10116 GN=Sf1 PE=1 SV=2	F1LSC3	Sf1	68 kDa		0.013
80	N-myc downstream regulated gene 2, isoform CRA_b OS=Rattus norvegicus OX=10116 GN=Ndrg2 PE=1 SV=1	A0A0G2JS...	Ndrg2	39 kDa		0.015
81	Brain acid soluble protein 1 OS=Rattus norvegicus OX=10116 GN=Basp1 PE=1 SV=2	Q05175	Basp1	22 kDa	★	0.015
82	Complexin-2 OS=Rattus norvegicus OX=10116 GN=Cplx2 PE=1 SV=1	P84087	Cplx2	15 kDa		0.015
83	RCG34610, isoform CRA_c OS=Rattus norvegicus OX=10116 GN=Srsf1 PE=1 SV=1	D4A9L2	Srsf1	28 kDa		0.015
84	Heterogeneous nuclear ribonucleoprotein H OS=Rattus norvegicus OX=10116 GN=Hnrnph1 PE=1 SV=1	A0A0G2JTG7	Hnrnph1	49 kDa	★	0.016
85	Heterogeneous nuclear ribonucleoprotein A3 OS=Rattus norvegicus OX=10116 GN=Hnrnpa3 PE=1 SV=1	Q6URK4	Hnrnpa3	40 kDa	★	0.016
86	Glutamine synthetase OS=Rattus norvegicus OX=10116 GN=Glul PE=1 SV=3	P09606	Glul	42 kDa		0.016
87	ATP synthase protein 8 OS=Rattus norvegicus OX=10116 GN=ATP8 PE=3 SV=1	Q5UAJ5	ATP8	8 kDa		0.017
88	RALY heterogeneous nuclear ribonucleoprotein OS=Rattus norvegicus OX=10116 GN=Raly PE=1 SV=2	E9PTI6 (+1)	Raly	33 kDa		0.018
89	Vimentin OS=Rattus norvegicus OX=10116 GN=Vim PE=1 SV=2	P31000	Vim	54 kDa	★	0.018
90	Proteasome subunit beta type-1 OS=Rattus norvegicus OX=10116 GN=Psmb1 PE=1 SV=3	P18421 (+1)	Psmb1	26 kDa		0.018
91	Matrin-3 OS=Rattus norvegicus OX=10116 GN=Matr3 PE=1 SV=2	P43244	Matr3	94 kDa		0.019
92	Neural cell adhesion molecule 1 OS=Rattus norvegicus OX=10116 GN=Ncam1 PE=1 SV=1	P13596	Ncam1	95 kDa		0.019
93	Heat shock cognate 71 kDa protein OS=Rattus norvegicus OX=10116 GN=Hspa8 PE=3 SV=3	D4A4S3 (+1)	Hspa8	71 kDa	★	0.023
94	60S ribosomal protein L19 OS=Rattus norvegicus OX=10116 GN=Rpl19 PE=1 SV=1	P84100	Rpl19	23 kDa		0.023
95	60S ribosomal protein L7a OS=Rattus norvegicus OX=10116 GN=Rpl7a PE=4 SV=2	F1M013	Rpl7a	30 kDa	★	0.023
96	Sodium/potassium-transporting ATPase subunit alpha-1 OS=Rattus norvegicus OX=10116 GN=Atp1a1 PE=1 SV=1	P06685	Atp1a1	113 kDa	★	0.024
97	Plectin OS=Rattus norvegicus OX=10116 GN=Plec PE=1 SV=1	Q6S3A0	Plec	534 kDa	★	0.024
98	Syntaxin-12 OS=Rattus norvegicus OX=10116 GN=Stx12 PE=1 SV=1	A0A0G2JVB6	Stx12	32 kDa		0.025
99	Isoaspartyl peptidase/L-asparaginase OS=Rattus norvegicus OX=10116 GN=Asrgl1 PE=1 SV=1	Q8VI04	Asrgl1	34 kDa		0.027
100	Transcription intermediary factor 1-beta OS=Rattus norvegicus OX=10116 GN=Trim28 PE=1 SV=2	O08629	Trim28	89 kDa		0.027
101	Cleavage and polyadenylation specificity factor subunit 5 OS=Rattus norvegicus OX=10116 GN=Nudt21 PE=2 SV=1	B4F764	Nudt21	26 kDa		0.027
102	Proteasome subunit alpha type-1 OS=Rattus norvegicus OX=10116 GN=Psma1 PE=1 SV=2	P18420	Psma1	30 kDa		0.027

103	Clathrin light chain OS=Rattus norvegicus OX=10116 GN=Clta PE=2 SV=1	Q5PPP1	Clta	24 kDa		0.027
104	Aldo-keto reductase family 1 member B1 OS=Rattus norvegicus OX=10116 GN=Akr1b1 PE=1 SV=3	P07943	Akr1b1	36 kDa		0.028
105	Actin, alpha skeletal muscle OS=Rattus norvegicus OX=10116 GN=Acta1 PE=1 SV=1	P68136	Acta1	42 kDa	★	0.029
106	Nucleophosmin OS=Rattus norvegicus OX=10116 GN=Npm1 PE=1 SV=1	P13084	Npm1	33 kDa		0.029
107	Heterogeneous nuclear ribonucleoprotein F OS=Rattus norvegicus OX=10116 GN=Hnrnpf PE=1 SV=3	Q794E4	Hnrnpf	46 kDa		0.029
108	Superoxide dismutase [Cu-Zn] OS=Rattus norvegicus OX=10116 GN=Sod1 PE=1 SV=2	P07632	Sod1	16 kDa		0.029
109	Vinculin OS=Rattus norvegicus OX=10116 GN=Vcl PE=1 SV=1	P85972	Vcl	117 kDa		0.030
110	Protein-L-isoaspartate O-methyltransferase OS=Rattus norvegicus OX=10116 GN=Pcmt1 PE=1 SV=1	A0A140TAB9	Pcmt1	21 kDa		0.030
111	60S ribosomal protein L11 OS=Rattus norvegicus OX=10116 GN=Rpl11 PE=1 SV=2	P62914	Rpl11	20 kDa		0.031
112	Leucine-rich repeat-containing 47 OS=Rattus norvegicus OX=10116 GN=Lrrc47 PE=1 SV=2	F1LT49	Lrrc47	64 kDa		0.031
113	Protein disulfide-isomerase A3 OS=Rattus norvegicus OX=10116 GN=Pdia3 PE=1 SV=2	P11598	Pdia3	57 kDa		0.032
114	ARVCF, delta catenin family member OS=Rattus norvegicus OX=10116 GN=Arvcf PE=1 SV=1	B4F7F3	Arvcf	105 kDa		0.033
115	Heterochromatin protein 1-binding protein 3 OS=Rattus norvegicus OX=10116 GN=Hp1bp3 PE=1 SV=1	Q6P747	Hp1bp3	61 kDa		0.034
116	Acidic (Leucine-rich) nuclear phosphoprotein 32 family, member A OS=Rattus norvegicus OX=10116 GN=Anp32a PE=2 SV=1	Q5PPH9	Anp32a	29 kDa	★	0.035
117	Heterogeneous nuclear ribonucleoprotein D-like OS=Rattus norvegicus OX=10116 GN=Hnrnpdl PE=1 SV=1	Q3SWU3	Hnrnpdl	35 kDa	★	0.038
118	Peroxiredoxin-6 OS=Rattus norvegicus OX=10116 GN=Prdx6 PE=1 SV=3	O35244	Prdx6	25 kDa		0.038
119	Acyl-CoA-binding protein OS=Rattus norvegicus OX=10116 GN=Dbi PE=1 SV=3	P11030	Dbi	10 kDa	★	0.040
120	Ras-related C3 botulinum toxin substrate 1 OS=Rattus norvegicus OX=10116 GN=Rac1 PE=1 SV=1	A0A0G2K0...	Rac1	24 kDa		0.040
121	Similar to RIKEN cDNA 2310022B05 OS=Rattus norvegicus OX=10116 GN=RGD1559896 PE=1 SV=1	D3ZY47	RGD15...	36 kDa		0.040
122	Mitochondrial import receptor subunit TOM22 homolog OS=Rattus norvegicus OX=10116 GN=Tomm22 PE=1 SV=1	Q75Q41	Tomm...	15 kDa		0.041
123	Proteasome subunit alpha type OS=Rattus norvegicus OX=10116 GN=Psma5 PE=1 SV=1	Q6P9V6	Psma5	26 kDa		0.042
124	Protein disulfide-isomerase OS=Rattus norvegicus OX=10116 GN=P4hb PE=1 SV=2	P04785	P4hb	57 kDa		0.043
125	Phosphoglycerate mutase 1 OS=Rattus norvegicus OX=10116 GN=Pgam1 PE=1 SV=4	P25113	Pgam1	29 kDa	★	0.043
126	Prothymosin alpha OS=Rattus norvegicus OX=10116 GN=Ptma PE=1 SV=2	P06302	Ptma	12 kDa		0.045
127	Peptidylprolyl isomerase OS=Rattus norvegicus OX=10116 GN=Fkbp3 PE=1 SV=1	G3V6L9	Fkbp3	25 kDa		0.046
128	Heterogeneous nuclear ribonucleoprotein D0 OS=Rattus norvegicus OX=10116 GN=Hnrnpd PE=1 SV=2	Q9JJ54	Hnrnpd	38 kDa		0.048
129	Microtubule-associated protein OS=Rattus norvegicus OX=10116 GN=Map2 PE=1 SV=3	F1LNK0	Map2	211 kDa	★	0.049